Title:

Episomal Tools for RNAi in the Diatom *Phaeodactylum tricornutum*

Authors:

Vincent A. Bielinski (1), Tayah M. Bolt (1), Christopher L. Dupont (2), and Philip D. Weyman (1)

Affiliations:

(1) Synthetic Biology and Bioenergy Group. J. Craig Venter Institute. La Jolla, CA, USA.
(2) Microbial and Environmental Genomics Group. J. Craig Venter Institute. La Jolla, CA, USA.

Correspondence:

Philip D. Weyman, pweyman@jcvi.org

PeerJ Preprints | https://doi.org/10.7287/peerj.preprints.2907v1 | CC BY 4.0 Open Access | rec: 4 Apr 2017, publ: 4 Apr 2017

Abstract

Background. The diatom *Phaeodactylum tricornutum* is a model photosynthetic organism. Functional genomic work in this organism has established a variety of genetic tools including RNA interference (RNAi). RNAi is a post-transcriptional regulatory process that can be utilized to knockdown expression of genes of interest in eukaryotes. RNAi has been previously demonstrated in *P. tricornutum*, but in practice the efficiency of inducing RNAi is low.

Methods. We developed an efficient method for construction of inverted repeat hairpins based on Golden Gate DNA assembly into a Gateway entry vector. The hairpin constructs were then transferred to a variety of destination vectors through the Gateway recombination system. After recombining the hairpin into the destination vector, the resulting expression vector was mobilized into *P. tricornutum* using direct conjugation from *E. coli*. Because the hairpin expression vectors had sequences allowing for episomal maintenance in *P. tricornutum*, we tested whether a consistent, episomal location for hairpin expression improved RNAi induction efficiency.

Results. We successfully demonstrated that RNAi could be induced using hairpin constructs expressed from an episome. After testing two different reporter targets and a variety of hairpin sequences with 3 polymerase II and 2 polymerase III promoters, we achieved a maximal RNAi induction efficiency of 25% of lines displaying knockdown of reporter activity by 50% or more. We created many useful genetic tools through this work including Gateway destination vectors for *P. tricornutum* expression from a variety of polymerase II and III promoters including the *P. tricornutum FCPB*, *H4*, and 49202 polymerase II promoters as well as the *U6* and *snRNA* polymerase III promoters. We also created Gateway destination vectors that allow a cassette cloned in an entry vector to be easily recombined into a transcriptional fusion with either ShBle or, for polymerase III promoters, the green fluorescent Spinach aptamer. Such transcriptional fusions allow for linkage of expression with a marker such as bleomycin resistance or fluorescence from the Spinach aptamer to easily select or screen for lines that maintain transgene expression.

Discussion. While RNAi can be used as an effective tool for *P. tricornutum* genetics, especially where targeted knockouts may be lethal to the cell, induction of this process remains low efficiency. Techniques resulting in higher efficiency establishment of RNAi would be of great use to the diatom genetics community and would enable this technique to be used as a forward genetic tool for discovery of novel gene function.

PeerJ Preprints | https://doi.org/10.7287/peerj.preprints.2907v1 | CC BY 4.0 Open Access | rec: 4 Apr 2017, publ: 4 Apr 2017

Introduction

Diatoms are globally distributed microalgae of great ecological and biotechnological importance (Nelson et al., 1995; Bozarth, Maier & Zauner, 2009; Hildebrand et al., 2012). While diatom genome sequences have enabled metabolic and evolutionary insights (Armbrust et al., 2004; Bowler et al., 2008; Mock et al., 2017), most genes are only functionally annotated through homology, and thousands of annotated genes have minimal or no functional verification. Use of RNA interference in diatoms to interrogate gene function was first enabled in the diatom model organism *Phaeodactylum tricornutum* by expression knockdown using hairpin- and antisense-RNA constructs (De Riso et al., 2009). Since this initial report, RNAi methods have been used in many studies to test the function of genes. Some examples include knockdown of proteins related to photo stress (Bailleul et al., 2010), of the ornithine-urea cycle protein carbamoyl phosphate synthetase I (Allen et al., 2011) and of proteins involved in lipid catabolism (Trentacoste et al., 2013). More recently, methods using targeted nucleases such as TALEN (Transcription activator-like effector nucleases) and CRISPR-Cas (Clustered Regulatory Interspaced Short Palindromic Repeats)/CRISPR-associated) allow for stable knockouts to be created to test the functions of genes of interest (Daboussi et al., 2014; Weyman et al., 2015; Nymark et al., 2016).

While many reverse genetic tools have been developed for diatoms as noted above, forward genetic tools have not yet been well established despite their clear promise for functionally characterizing genes (Alonso & Ecker, 2006). Forward genetic approaches target genes for knockdown or knockout in a more or less random manner and identify phenotypes that can then be studied genetically to identify the causal lesion(s). In a forward genetic approach, the genes resulting in the phenotype of interest are not necessarily known *a priori*. The ability to install RNAi efficiently would enable its use as a "forward" genetic tool by allowing the use of libraries of RNAi constructs that could be used to transform *P. tricornutum* cells. The resulting phenotypes of interest could be selected and the targets of the RNAi constructs would point to the genes responsible for the phenotype when disrupted. Such RNAi libraries have been used successfully in other systems including *Caenorhabditis elegans* (Kamath et al., 2003) and human cells (Berns et al., 2004). Using RNAi libraries as a forward genetic approach in *P. tricornutum* would have the benefit of functioning post-transcriptionally to avoid challenges obtaining biallelic (homozygous) mutants in a diploid organism with no observed sexual cycle. However, for such RNAi libraries to be used effectively for forward genetic screens, efficiency of successful RNAi establishment and nuclear transformation must both be high to test large, complex libraries.

We hypothesized that the requirement for random integration of the expression cassette in the genome may have limited the resulting hairpin expression and reduced the efficiency of RNAi in its previous applications in *P. tricornutum*. If a limiting factor in RNAi delivered by biolistic transformation is inconsistent expression of the hairpin due to position effects of random

PeerJ Preprints | https://doi.org/10.7287/peerj.preprints.2907v1 | CC BY 4.0 Open Access | rec: 4 Apr 2017, publ: 4 Apr 2017

integration, then a more consistent genomic environment for its expression may lead to a higher probability of knockdown success. Recently, the development of episomal vectors in diatoms delivered directly by conjugation from *E. coli* offers an alternative platform for expression of RNAi constructs (Karas et al., 2015; Diner et al., 2016a). We sought to test whether a more stable and consistent platform for expression could enable more efficient establishment of RNAi in *P. tricornutum*.

We also hypothesized that driving expression of the hairpin construct from a polymerase III (pol III) promoter such as U6 may improve efficiency of RNAi induction. In animals, RNAi has been achieved by expression of short hairpin RNA (shRNA) constructs from either polymerase II or III promoters (Lee et al., 2004; Borchert, Lanier & Davidson, 2006). In contrast, plants typically express small RNAs from polymerase II (pol II) promoters (Axtell, Westholm & Lai, 2011). There are many differences in the processing, transport, and regulation of transcripts produced by RNA polymerase II or III (Fuda, Ardehali & Lis, 2009; Turowski & Tollervey, 2016). Since expression of hairpin RNA in *P. tricornutum* has only been reported with polymerase II promoters, it is unknown whether expression of hairpin RNAs from polymerase III promoters that are responsible for transcribing non-coding small RNAs would lead to improved RNAi in *P. tricornutum*.

In this paper, we present the first demonstration of RNAi with hairpin constructs expressed from an episome. We observe successful expression knockdown of yellow fluorescent protein (*YFP)* and beta-glucuronidase (*GUS)* reporter genes after introducing episomes encoding RNAi cassettes. We tested promoters of different strengths and polymerase type and designed strategies to maintain hairpin expression through transcriptional fusions with markers. Delivering RNAi constructs to *P. tricornutum* on an episome by conjugation required substantially less time and fewer resources to complete the experiments than with previous biolistic transformation approaches. However, the frequency of RNAi induction remained lower than required to use this technique for efficient genome-wide, forward genetic screens.

Materials and Methods

Generation of a constitutive GUS-expressing strain

Plasmid pPtRNAi-2c, a plasmid to constitutively express GUS with a nourseothricin resistance marker, was constructed from three PCR products. To generate the first product, we first replaced the ShBle coding region in pPtPBR2 (non-maintained in *P. tricornutum*) with that of the nourseothricin resistance gene to create pPtRNAi5. This was performed by amplifying the nourseothricin resistance gene with primers PtRNAi-7 + PtRNAi-8 (See Supplemental Table 1 for all primer sequences) and amplifying the pPtPBR2 backbone to exclude the ShBle coding region with primers BackF + BackR and assembling the two products by Gibson assembly. Then, the first product used to construct pPtRNAi2c that included the portion of the vector including the nourseothricin resistance cassette, the plasmid origin for *E. coli*, and the ampicillin

PeerJ Preprints | https://doi.org/10.7287/peerj.preprints.2907v1 | CC BY 4.0 Open Access | rec: 4 Apr 2017, publ: 4 Apr 2017

resistance gene was amplified by primers PtRNAi-32 + PBR-nanoluc-4. The second fragment of the assembly of pPtRNAi-2c was amplified as part of pPtPBR2 vector (including the TetR and the oriT) that was pre-assembled with the *P. tricornutum* FcpB promoter *(pFcpB)*. This was performed by amplifying the vector with primers PBR-nanoluc-5 + and PtRNAi-31 and amplifying *pFcpB* with primers PtRNAi-25 + PtRNAi-29 and using the PCR-added sequence overlaps to assemble the two amplified products by PCR. After pre-assembly, the product was amplified with the flanking primers PBR-nanoluc5 and PtRNAi25. The third fragment for the assembly of pPtRNAi-2c was the GUS open reading frame that was pre-assembled to the *P. tricornutum* FcpA terminator. This was performed by amplifying the GUS open reading frame with primers PtRNAi-26 + PtRNAi-27 and the FcpA terminator with primers PtRNAi-28 + PtRNAi-30 and pre-assembling by PCR. After pre-assembly, the product was amplified with the flanking primers PtRNAi-26 + PtRNAi-30.

After the sequence of plasmid PtRNAi-2c was verified by Sanger DNA sequencing, it was introduced into wild type *P. tricornutum* using biolistic transformation with the PDS-1000 system (Apt, Kroth-Pancic & Grossman, 1996) and colonies selected on ½x L1-agar plates supplemented with 200 µg mL^{-1} nourseothricin (GoldBio) plates. Colonies were then screened for the presence of the GUS gene via colony PCR and subjected to enzymatic assay to determine positive strains. One *P. tricornutum* GUS-expressing line, G1-16, was selected as the recipient for introduction of hairpin expression plasmids.

Generation of a constitutive YFP-expressing strain

Plasmid pPtRNAi-1c was created to express YFP from *pFcpB* and selected in *P. tricornutum* with nourseothricin resistance. The plasmid backbone was amplified using pPtRNAi5 as a template with primers Ptrnai-31 + Ptrnai-32. This product was assembled with a FcpB-YFP fragment amplified from pPtPBR1-YFP-CENH3 (Diner et al., 2016b) using primers Ptrnai-29 + PtRNAi22, and the FcpA terminator amplified from the same template using primers PtRNAi-23 and PtRNAi-30. The assembled plasmid was verified by Sanger DNA sequencing and introduced into *P. tricornutum* using biolistic transformation as described for the GUS-expressing lines.

Construction of Destination Vectors

Destination vectors containing Pol II promoter/terminator pairs were constructed using the Gibson assembly method. DNA fragments corresponding to the FcpB (pFcpB-DEST), H4 (pH4-DEST), and 49202 (p49202-DEST), and NR (pNR-DEST) 5'-UTRs were amplified from *P. tricornutum* genomic DNA and assembly was carried out via Gibson method.

Plasmid pFcpB-DEST was designed to be a destination vector that allowed for insertion of the hairpin downstream of the *P. tricornutum* FcpB promoter (434-bp preceding PHATRDRAFT_25172) and was assembled from three fragments amplified by PCR. The first fragment amplified the FcpB promoter- AttR1-CatR-ccdB-AttR2-FcpA terminator using plasmid pDest-OX as a template (Siaut et al., 2007) using primers Ptrnai-3 + Ptrnai-4. The second

PeerJ Preprints | https://doi.org/10.7287/peerj.preprints.2907v1 | CC BY 4.0 Open Access | rec: 4 Apr 2017, publ: 4 Apr 2017

product was amplified with primers Ptrnai-5 + PBR-nanoluc4 using pPtPBR1 as a template (Karas et al., 2015) and the third product was amplified with primers PBR-nanoluc5 + Ptrnai-6 using pPtPBR1 as a template.

Plasmid pH4-DEST allowed for expression of the hairpin from the *P. tricornutum* H4 promoter (655-bp preceding PHATRDRAFT_26896) and p49202-DEST allowed for expression of the hairpin from the region of DNA upstream of the ATG site for *P. tricornutum* gene 49202 (1,521-bp preceding PHATRDRAFT_49202). The first PCR product for pH4-DEST was amplified using Ptrnai-47 and Ptrnai-48 using *P. tricornutum* genomic DNA as a template. Products 2 and 3 were amplified using Ptrnai-49 + Ptrnai-50 and Ptrnai-51 + Ptrnai-52.2, respectively, using pPtPBR1 as a template. To create plasmid p49202-DEST, products 2 and 3 were identical, while product 1 was amplified using primers Ptrnai-53 + Ptrnai-54 using *P. tricornutum* genomic DNA as a template.

For the direct transcriptional fusion of the hpRNA to the mRNA encoding ShBle, we utilized the diatom conjugation vector pPtPBR1 (Karas et al., 2015) as a template to assemble the DEST cassette at either side of the ShBle resistance marker. These vectors therefore use the FcpF promoter (687-bp preceding PHATRDRAFT_51230) and FcpA terminator for expression of both the hairpin and the ShBle cassette on the same transcript. To create a destination vector in which the hairpin was expressed 5' (upstream) of the ShBle coding region, the vector (plasmid pPtPBR-1) was amplified by PCR using primers (shBle-F + fcpF pro-R) and the DEST cassette (including AttR1-CatR-ccdB-AttR2 sites) was amplified using primers (5'fusion-shBle-DESTcasF + 5'fusion-shBle-DESTcasR). These PCR products were purified and assembled by Gibson Assembly to create plasmid p5'fusion-shble-DEST. To make a destination vector in which the hairpin was expressed 3' (downstream) of the ShBle coding region, the vector (plasmid pPtPBR-1) was amplified by PCR using primers (FcpA term-F + Backbone 40-R) and the DEST cassette (including AttR1-CatR-ccdB-AttR2 sites) was amplified using primers (shBle-3'fusion-DESTcasF + shBle-3'fusion-DESTcasR). These PCR products were purified and assembled by Gibson Assembly to create plasmid pshble-3'fusion-DEST.

To express the hairpins from Pol III promoters, we constructed destination vectors pU6-DEST and psnRNAi-DEST that will transcribe the hairpin from the U6 promoter (Nymark et al., 2016) and a newly discovered snRNA promoter, respectively (M. Moosburner and, A. E. Allen personal communication). To construct pU6-DEST, the native promoter and terminator for the U6 gene was amplified from *P. tricornutum* genomic DNA. Primers (U6-Pro-F and U6-Pro-R) were designed against a region of chromosome 8 at positions 239707-239986 (promoter) and primers for the terminator (U6 term-F and U6 term-R) were designed against positions 239267-239596 to amplify fragments for the U6 DEST vectors. To construct psnRNAi-DEST, primers (snRNAiPro-F and snRNAiPro-R) were designed against a region of chromosome 2 at positions 28039-29038 to amplify the promoter and primers snRNAiterm-F and snRNAiterm-R were used

PeerJ Preprints | https://doi.org/10.7287/peerj.preprints.2907v1 | CC BY 4.0 Open Access | rec: 4 Apr 2017, publ: 4 Apr 2017

to amplify positions 29124-29423 for the terminator. Plasmid PtRNAi-3 was used as a template for generation of two backbone fragments, each one containing a resistance marker. The tetR fragment was generated using primers Backbone-33-F and snRNAi-DEST-BB-R, while the ampR-containing fragment was generated with primers Backbone-34 and Backbone-35. The DEST cassette was amplified using primers snRNAI-DEST-BB-F and DEST-cas-R. To construct pU6-DEST, plasmid PtRNAi-3 was again used as a template for backbone fragments, with the ampR fragment amplified with primers Backbone 37-R and Backbone-shble-F while the tetR fragment was amplified using primers Backbone 38-F and U6-Backbone 39-R. The DEST cassette fragment was generated using primers U6-DEST-cas-F and U6-DEST-cas-R. The appropriate PCR products were then assembled using Gibson Assembly to generate pU6-DEST and psnRNAi-DEST.

To construct destination vectors featuring the U6 promoter driving a transcriptional fusion between the hairpin and the fluorescent "Spinach" aptamer, the fragment corresponding to the 135-bp Spinach2 aptamer (Strack, Disney & Jaffrey, 2013) was synthesized as two separate ultramers (Spinach2-sense and Spinach2-antisense) by IDT which were annealed in-house. This fragment was then used as a template for PCR amplification with the appropriate primers to build destination vectors p5'-Spinach-DEST and p3'-Spinach-DEST vectors. To create p5'-Spinach-DEST, the Spinach aptamer was amplified with primers U6-5'-Spinach-F + U6-5'-Spinach-R and the DEST cassette amplified from PtRNAi-3 with primers U6-5'Spinach-DESTcasF + U6-DEST-cas-R. The U6 promoter was amplified from pU6-DEST using primers U6-pro-F and U6 Pro-R-5'Spinach and the terminator amplified from the same template with primers U6 term-F-noOH and U6 term-R. To create p3'-Spinach-DEST, the Spinach aptamer was amplified with primers (U6-3'-Spinach-F + U6-3'-Spinach-R) and the DEST cassette amplified from PtRNAi-3 with primers U6-DEST-cas-F + U6-DEST-3'Sp-cas-R. The U6 promoter and terminator were amplified from pU6-DEST using primers U6-Pro-F + U6-Pro-R (promoter) and U6-term-3'Sp-F + U6 term-R (terminator). The two PCR products used to create the resistance marker-containing fragments from the construction of pU6-DEST were re-used in the construction of both fusion vectors. For both plasmids, PCR products were purified and assembled using Gibson Assembly.

Plasmids pPtGG-1, pFcpB-DEST, pH4-DEST, p49202-DEST, pNR-DEST, pU6-DEST, psnRNA-DEST, p5'fusion-shble-DEST, pshble-3'fusion-DEST, p5'-Spinach-DEST, and p3'-Spinach-DEST will be made available from the plasmid repository Addgene at the time of publication.

Assembly of hairpins - The hpRNA entry vectors were assembled via the Golden Gate method (Engler, Kandzia & Marillonnet, 2008). An overview and detailed protocol for how to create Golden Gate primers can be found at Protocols.io (dx.doi.org/10.17504/protocols.io.heyb3fw). We first constructed an entry vector (called "pPtGG-1") consisting of a pBR322 backbone in

PeerJ Preprints | https://doi.org/10.7287/peerj.preprints.2907v1 | CC BY 4.0 Open Access | rec: 4 Apr 2017, publ: 4 Apr 2017

which the ampicillin resistance cassette was deleted and replaced with attL sites flanking a non-coding region of DNA consisting of two multiple cloning sites separated by a portion of the "white" intron from Drosophila (Engler, Kandzia & Marillonnet, 2008) that should not form hairpin DNA when transcribed. This region was later used as a negative control sequence that lacked both a target in the *P. tricornutum* chromosome and a hairpin structure (see below). To create pPtGG-1, two ultramers comprising the spacer region were synthesized by IDT (PtGG-1 "MCS" Ultramer F and PtGG-1 "MCS" Ultramer R) which were annealed in-house and assembled into pENTR-d-TOPO (Invitrogen) using the manufacturer's protocol. The region encoding AttL1-Spacer-AttL2 was amplified using primers 5'hpRNA-F-OH and 3'hpRNA-R-OH and assembled by Gibson Assembly with the pBR322 backbone amplified as specified above using primers (5'hpRNA-F-vector and 3'hpRNA-R-vector) resulting in plasmid pPtGG-1. For use in assembling hairpin entry vectors, the backbone plasmid pPtGG-1 was amplified via PCR using the primers PtRNAi-43 and PtRNAi-44 with PrimeStar polymerase (Takara) to generate a roughly 3.5 kb fragment.

To construct hairpins targeting the *YFP* gene, PCR products between 180-360 bp in size making up the "left" and "right" arms of the hairpin were amplified from template pPtPBR-CENH3-YFP (Diner et al., 2016b) (Table 1). To construct hairpins targeting the GUS gene, the left and right "arms" that composed the inverted repeat hairpin were generated by amplifying 300-bp regions of the *GUS* gene using the plasmid pBI-121 (Chen et al., 2003) as template. Primers used to amplify the arms and the spacer attached BsaI sites that when digested would generate an overhang sequence that was unique to form the desired junction; three such junctions were created to join the three fragments (left and right arms and vector)(Table 2). The two arms composing the hairpin were separated by a (51 bp) spacer region (Wang et al., 2013), and each arm contained half of the spacer that was created by sequence added to the PCR primer. Successful joining of the two arms through Golden Gate assembly would create a sense/antisense hairpin with the complete spacer intron in between the two arms.

PCR products for each arm were first cleaned up using the QIAquick PCR cleanup kit (QIAGEN), removing salts, free nucleotides, and polymerase. This was followed by a further purification of the PCR products away from leftover unused primers by applying AMPure XP beads (Beckman Coulter) and following the manufacturer's instructions on basic cleanup of PCR products. Briefly, 1.8x volume beads suspension was added to fragment-containing eluate from QIAquick cleanup, then the beads were washed 2x with 70% EtOH and finally eluted into TE buffer, pH 8.0. This extra cleanup successfully removed excess primers from the PCR products.

Golden Gate Reaction - The PCR products for gene target ("arms") were diluted to 60 fmol μl^{-1} and PCR-amplified pPtGG- backbone to 20 fmol μL^{-1} using H_2O (3:1 final ratio in reaction of arms:vector). T4 ligase was diluted 1:200 into fresh T4 ligase buffer (final concentration 10U μL^{-1}). The reaction we optimized utilized CutSmart buffer (50mM Potassium Acetate, 20mM

PeerJ Preprints | https://doi.org/10.7287/peerj.preprints.2907v1 | CC BY 4.0 Open Access | rec: 4 Apr 2017, publ: 4 Apr 2017

Tris-acetate, 10mM Magnesium Acetate, and 100µg mL^{-1} BSA, pH 7.9, NEB). The final reaction mixture was 1x CutSmart Buffer, 1mM DTT, 1mM ATP, 6 fmol Arm1 fragment, 6 fmol, 2 fmol PtGG-43+44 PCR product, 5U BsaI-HF, and 10U T4 ligase in a total volume to 10 µL. The thermocycler parameters for assembly were 37°C for 1 min followed by 16°C for 1 min for a total of 30 cycles. A 5-minute 50°C final digest was added after cycling, followed by a 10-minute heat inactivation step at 65°C. Once finished, the samples were diluted 1:5 with ddH2O and 2 µl of diluted reaction was transformed into Epi-300 *E. coli* cells via electroporation. For all bacterial work during these studies, we chose to perform our outgrowths and incubations at 30°C to stabilize the assembled hairpins and prevent looping out of the inverted repeats while in the bacteria. The cells were then plated onto LB-Tet10 and incubated overnight at 30°C.

Colony PCR for Bacterial Cloning - Colonies were patched and screened for the presence of both arms in the assembled entry vector. Primers designed to amplify each arm utilized a flanking upstream or downstream site and a site in the intronic, spacer region as a unique primer binding site. The primer sets (called "Arm1" using primers F-OH + Riceintron1 and "Arm2" using primers R-OH and Riceintron2) were used in separate PCR reactions, as it is difficult to PCR across regions of inverted repeat DNA (such as hairpins). PCR reactions were performed using OneTaq (NEB) according to the manufacturer's recommended protocol.

LR reaction - Hairpins were transferred from entry vectors to destination vectors using the LR recombinase reaction (LR Clonase II, Life Technologies) according to the manufacturer's directions. After completion of the reaction, 1 µL was transformed into Epi-300 cells (Epicentre) and plated on LB with ampicillin (100 µg mL^{-1}) and tetracycline (10 µg mL^{-1}). All incubations of bacteria were carried out at 30° C. Resulting colonies were screened for the presence of both hairpins as described above.

Conjugation Protocol - Bacterial-mediated conjugation of episomes into the G1-16 strain (chromosomal integration of the FcpB promoter-GUS expression construct) were carried out in the 12-well format as described (Diner, et al 2016). After two days of recovery without selection, the cells in each well were scraped into 500 µL of L1 medium and the entire resuspension replated on a single 100mm ½x-L1 plate containing nourseothricin (200µg mL^{-1}) and phleomycin (20 µg mL^{-1}, abbreviated as ½xL1-N200-P20). Excess liquid from the added cells was allowed to dry with the plate open in a laminar flow hood. Selection plates were then incubated for 7-10 days at 21°C with 100 µmol photons $(m^2s)^{-1}$ light intensity and 16:8 day/night cycle. For constructs that provided low levels of exconjugants with the 12-well format, conjugation was repeated using the method described in Karas, et al (2015). After the selection plates cleared, colonies were picked and patched onto a fresh ½xL1-N200-P20 plate and further incubated until biomass was accumulated and subjected to screening.

PeerJ Preprints | https://doi.org/10.7287/peerj.preprints.2907v1 | CC BY 4.0 Open Access | rec: 4 Apr 2017, publ: 4 Apr 2017

Colony PCR Analysis of *P. tricornutum* Exconjugants - Colonies that continued to grow upon the patched selection plates were then subjected to colony PCR analysis using the Arm1 and Arm 2 primers design as described above for bacterial screening; however, the R-OH primer was replaced with RNAi3-DR (which resides in the FcpA terminator sequence). Colonies were screened for the presence of Arm 1 and Arm 2 of the hpRNA construct in separate reactions using the same OneTaq conditions as described above for bacteria, except for the addition of 5 extra PCR cycles (total of 30 cycles for P. tricornutum colonies). Colonies that gave positive results for both arms of the hpRNA episome were then scraped into 2 mL of liquid L1-N200-P20 and incubated at 21°C with 100 µmol photons m2-1 s-1 light intensity and 16:8 day/night cycle. For analysis of GUS knockdown, these cultures were then scaled up and analyzed as described below.

YFP Plate Assay - Cultures were grown in L1 supplemented with 200 µg mL^{-1} nourseothricin (Gold Bio) at 18°C at 100 µM in 2 mL cultures in a 24-well tissue culture plate. On the day of the assay, the plate was analyzed using a Flexstation 3 (Molecular Devices) and the optical densities of the cultures were measured at 750 nm. Chlorophyll (Chl) fluorescence was then measured, using 436nm and 680nm (665nm auto-cut-off) as excitation and emission wavelengths, respectively. YFP fluorescence was measured using 486 nm and 530 nm (515nm auto-cutoff) as excitation and emission wavelengths, respectively. The YFP fluorescence was normalized by dividing by the Chl fluorescence for each well. This value was then divided by the OD750 values for the same well and recorded as (YFP Chl^{-1})OD^{-1}.

GUS Assay - Cultures were grown in L1 medium supplemented with 200 µg mL^{-1} nourseothricin (Gold Bio) at 21°C at 100 µm in 5 mL cultures to an approximate density of 3-4x10^6 cells mL^{-1}. On the day of the assay, cells were harvested by centrifugation for 10 minutes at 3,000 g. The supernatant was poured off and the cell pellet was resuspended in 200 µL of freshly made GUS extraction buffer (50mM NaPO4, pH 7, 0.1% Triton X-100, 10 µM beta-mercaptoethanol) and subjected to three freeze/thaw cycles. The lysates were then clarified with a 5-minute spin at 4°C at 15,000 g. The supernatant was then transferred to a new 1.5 mL Eppendorf tube and stored on ice. For the assay, 25 µL of supernatant was added to 475 µL of pre-warmed GUS extraction buffer containing 1 mM MUG (4-Methylumbelliferyl beta-D-glucuronide) and incubated at 37°C for 90 minutes. 100 µL of the assay sample was then added to 900 µL of "stop" buffer (0.2M Na_2CO_3) and mixed. 200 µL of the quenched assay sample was then transferred to an opaque 96-well plate and fluorescence was measured using a FlexStation 3 plate reader with excitation/emission settings of 360 nm excitation/440 nm emission (cutoff at 435nm). For normalization, 10 µL of the original clarified lysate was subjected to a BCA assay (ThermoFisher) and the amount of total protein added to each assay well was calculated and used for normalization and final numbers were determined as RFU $µg^{-1}$ total protein. Blank wells using only GUS extraction buffer were added as "blanks" for each plate reader assay. The complete protocol can be found at protocols.io (dx.doi.org/10.17504/protocols.io.hefb3bn)

PeerJ Preprints | https://doi.org/10.7287/peerj.preprints.2907v1 | CC BY 4.0 Open Access | rec: 4 Apr 2017, publ: 4 Apr 2017

Results

We developed an efficient method to build hairpins based on Golden Gate cloning (dx.doi.org/10.17504/protocols.io.heyb3fw) using YFP and GUS as efficient test reporters for induction of RNA interference (RNAi). Hairpins were first assembled into Gateway system entry vectors, and the hairpin was then recombined into a destination vector resulting in a hairpin expression vector (Fig. 1A). Because the episomal expression of hairpin vectors to induce RNAi has never been reported for *P. tricornutum*, we developed a workflow of colony PCR checks at every transfer point to ensure that the hairpin expression construct was successfully maintained and delivered to *P. tricornutum* and was not lost due to recombination (Fig. 1B). This involved confirming the presence of both hairpin arms by colony PCR after construction of the expression plasmid, after moving the plasmid to the *E. coli* strain for conjugation, and in *P. tricornutum* lines after conjugation. Over 95% of *P. tricornutum* lines tested were positive by PCR for the presence of both hairpin arms.

We first targeted YFP for knockdown using a reporter line that constitutively expressed YFP from a native chromosomal location. Into this YFP reporter line we introduced episomes with one of four different hairpin expression cassettes targeting different parts of the YFP coding region. The hairpins were expressed from the FcpB promoter. The hairpins varied in length from 180 bp (*P. tricornutum* lines Exp 1 and Exp 2) to 360 bp (lines Exp 3 and Exp 4), and after introduction of the episomes into a YFP-expressing *P. tricornutum* line, 8 resulting lines were screened as described above and tested for YFP fluorescence. Variability of the YFP-expressing reporter line without knockdown was estimated after introducing an empty vector control episome (Fig. 2). Of the 32 lines tested in which hairpin expression vectors were introduced, 6 displayed reductions in YFP fluorescence greater than one standard deviation of the empty vector control, a knockdown success rate of 18%.

While YFP was an easily detectable and convenient target to screen for RNAi knockdown, the relatively high background fluorescence of the *P. tricornutum* cells made it difficult to accurately assess the full extent of knockdown. To circumvent this problem, we switched the targeted reporter to the beta-glucuronidase gene (*GUS*). Using the fluorescent substrate 4-methylumbelliferyl-β-D-glucuronide hydrate (MUG), background activity in wild type *P. tricornutum* was very low, and high signal to noise measurements could be obtained.

We divided the 1,812 bp *GUS* gene into six ~300-bp regions and constructed hairpin entry vectors for each. These entry vectors were then used to create six different hairpin expression vectors for each of five different promoters: polymerase II promoters FcpB, 49202, or H4 and polymerase III promoters U6 or snRNA. Each of these 30 unique promoter-hairpin constructs was introduced into a GUS-expressing reporter line, screened for the presence of hairpin

PeerJ Preprints | https://doi.org/10.7287/peerj.preprints.2907v1 | CC BY 4.0 Open Access | rec: 4 Apr 2017, publ: 4 Apr 2017

maintenance, and tested for GUS activity. Six lines for each of the 30 constructs were tested for GUS activity; controls including the parental GUS-expressing line and a negative control lacking GUS expression were included for each assay. Overall, we found a relatively low rate of RNAi formation with just 14% of FcpB driven hairpin lines displaying a knockdown phenotype of 50% of parental GUS activity or less (Fig. 3A). Knockdown success was somewhat higher at 25% for the 49202-driven hairpins (Fig. 3B). Only 2 knocked down lines (5.6 %) were observed using the H4 promoter to drive hairpins (Supplemental Figure 1). Some hairpin cassettes appeared to provide better knockdown than others but no consistent trend was observed across different promoters. We also tested the ability of the polymerase III promoters U6 and snRNA to drive hairpin expression and found that each promoter successfully knocked down GUS expression by 50% in 14% of lines which was similar to knockdown by polymerase II promoters FcpB and 49202.

In an attempt to improve RNAi knockdown efficiency, we constructed four new vectors that allowed for continuous selection or screening for hairpin expression. The first two vectors were constructed as destination vectors using the FcpB promoter to drive a transcriptional fusion between the hairpin and the coding region of the ShBle bleomycin resistance gene (Fig. 4). In one vector (Exp 40-44) the hairpin was 5' (upstream) of the ShBle and in the other vector (Exp 52-56), the hairpin was located 3' (downstream) of the ShBle cassette. When the hairpin came first on the transcript, a strong Kozak sequence was included before the ShBle coding region. The second approach of expressing the hairpin after the ShBle cassette as a transcriptional fusion was previously reported with success (De Riso et al., 2009).

Results for ShBle transcriptional fusions are forthcoming in a future draft.

Because polymerase III promoters cannot be used to express protein coding genes, we chose to fuse hairpin transcription with that of the fluorescent aptamer, Spinach, to allow cells that maintained expression to be screened. We constructed two versions of the U6 promoter driving a transcriptional fusion between the hairpin and the spinach aptamer. The first (Exp 52-56) expresses the hairpin 5' (upstream) of the aptamer and the second (Exp 58-62) expresses the aptamer first followed by the hairpin 3' (downstream) of the aptamer (Fig. 4).

Results for Spinach tests and transcriptional fusions are forthcoming in a future draft.

Discussion:

We successfully knocked down reporter gene expression in *P. tricornutum* by expressing inverted repeat hairpins on stable episomes. Knockdown was somewhat improved when hairpins were expressed with the stronger promoter from *P. tricornutum* gene 49202 (25% of tested lines with knockdown) compared to the FcpB promoter (14% of tested lines with knockdown). The

PeerJ Preprints | https://doi.org/10.7287/peerj.preprints.2907v1 | CC BY 4.0 Open Access | rec: 4 Apr 2017, publ: 4 Apr 2017

49202 promoter is one of the highest expressed genes in *P. tricornutum* (Chen et al., 2003). Detailed analysis of the promoter activities will be presented in a forthcoming manuscript (Bielinski et al. in preparation). We found no improvement in knockdown frequency when polymerase III promoters were used in place of the standard, previously reported polymerase II promoters (De Riso et al., 2009) to drive hairpin expression. Overall, our data allows us to reject our hypothesis that knockdown frequency in *P. tricornutum* could be improved by hairpin expression from a stable episomal location. This points to other factors other than hairpin expression that need to be further optimized in *P. tricornutum* to improve RNAi establishment frequency.

Even when hairpins are expressed from episomal locations, it is possible that the cell could be very sensitive to hairpin expression and may downregulate hairpin expression epigenetically. To eliminate this possibility, we constructed transcriptional fusions such that the hairpin would be co-transcribed with a selectable or fluorescent marker protein to allow cells with active hairpin expression to be identified. Essentially, these vectors directly couple a selectable marker to expression of the hairpin; cells that lose expression of the hairpin would also lose expression of the marker. By coupling selection with hairpin expression, we can ensure that the hairpin is not being repressed during growth. This strategy was successful in previously reported work (De Riso et al., 2009)), but we were able to identify knockdown lines in using transcriptional fusions to the ShBle coding region.

Two versions of the transcriptional fusions to ShBle were created. In the first version (the design previously reported, (De Riso et al., 2009)), ShBle was expressed first followed by the hairpin. While we ensured that both arms of the hairpin were located on the episome after delivery to *P. tricornutum*, it was unclear if the hairpin was successfully expressed or if transcription through the hairpin was halted prematurely. In the second version in which the hairpin was located upstream of the ShBle selectable marker, we recovered very few colonies (roughly 1,000-fold fewer than for the first version where ShBle preceded the hairpin). Thus, it would seem that the hairpin preceding the ShBle prohibited expression of the selectable marker by some mechanism.

At least three mechanisms may be hypothesized as to why hairpins located upstream of the ShBle coding region prevented expression of selectable marker. First, the inability to co-express the ShBle gene when the hairpin was located before the selectable marker open reading frame may suggest that the hairpin is terminating transcription. While hairpin-mediated transcriptional termination is a common phenomenon in bacteria, we could find no evidence for this in eukaryotes in the literature. Second, if transcription is not terminating, then perhaps cleavage of the hairpin by the DICER RNase renders the remaining portion of the transcript containing the ShBle unable to be translated. Problems with translation of this internal ShBle coding region may occur even if efficient cleavage of the hairpin is not occurring despite the presence of a strong Kozak sequence before the ShBle. A third hypothesis is that the hairpin is being

PeerJ Preprints | https://doi.org/10.7287/peerj.preprints.2907v1 | CC BY 4.0 Open Access | rec: 4 Apr 2017, publ: 4 Apr 2017

transcribed, and the expression cassette is immediately targeted for epigenetic downregulation of transcription (e.g. via methylation). Such RNA directed DNA methylation (RdDM) was previously shown to be triggered by RNAi for the GUS reporter gene in *P. tricornutum* (De Riso et al., 2009). However, whether the hairpin expression cassette itself was targeted by RdDM was never tested, and it may be hypothesized that *P. tricornutum* lines that fail to induce RNAi may have silenced expression from the hairpin rather than the reporter gene. Overall, such methods may be helpful to keep the hairpin and selectable marker as tightly linked as possible as rearrangements frequently occur during biolistic transformation. However, we did not find that this method helped select for continuously active RNAi when the hairpin was expressed from the episome.

Conclusions:

We have thoroughly tested methods to establish RNAi-mediated transcriptional knockdown using episome-based hairpin expression cassettes in *P. tricornutum*. By testing three polymerase II promoters, two polymerase III promoters, two different knockdown targets, a variety of hairpin sequences and lengths, and hairpins expressed as transcriptional fusions, we conclude that factors other than a stable platform for hairpin expression remain limiting for high efficiency knockdown in *P. tricornutum*.

Acknowledgements:

The authors acknowledge Josefa Rivera for assistance with laboratory techniques supporting this paper. We are grateful to Mark Moosburner and Andrew E. Allen for allowing us to use the snRNA promoter location that they identified.

Author Contributions:

V.A.B, C.L.D, P.D.W conceived of experiments and approaches, V.A.B, T.M.B, P.D.W performed experiments, V.A.B, T.M.B, C.L.D, P.D.W analyzed data, and V.A.B, C.L.D, P.D.W wrote the manuscript.

Funding Statement:

Funding for this work was provided by the Gordon and Betty Moore Foundation (GBMF5007 to P.D.W. and C.L.D.).

References:

Allen AE., Dupont CL., Oborník M., Horák A., Nunes-Nesi A., McCrow JP., Zheng H., Johnson D a., Hu H., Fernie AR., Bowler C. 2011. Evolution and metabolic significance of the urea cycle in photosynthetic diatoms. *Nature* 473:203–207. DOI: 10.1038/nature10074.

Alonso JM., Ecker JR. 2006. Moving forward in reverse: genetic technologies to enable genome-wide phenomic screens in Arabidopsis. *Nature reviews. Genetics* 7:524–536. DOI: 10.1038/nrg1893.

Apt KE., Kroth-Pancic PG., Grossman AR. 1996. Stable nuclear transformation of the diatom Phaeodactylum tricornutum. *Mol Gen Genet* 252:572–9.

Armbrust EV., Berges JA., Bowler C., Green BR., Martinez D., Putnam NH., Zhou S., Allen AE., Apt KE., Bechner M., Brzezinski MA., Chaal BK., Chiovitti A., Davis AK., Demarest MS., Detter JC., Glavina T., Goodstein D., Hadi MZ., Hellsten U., Hildebrand M., Jenkins BD., Jurka J., Kapitonov V V., Kröger N., Lau WWY., Lane TW., Larimer FW., Lippmeier JC., Lucas S., Medina M., Montsant A., Obornik M., Parker MS., Palenik B., Pazour GJ., Richardson PM., Rynearson TA., Saito MA., Schwartz DC., Thamatrakoln K., Valentin K., Vardi A., Wilkerson FP., Rokhsar DS. 2004. The genome of the diatom Thalassiosira pseudonana: ecology, evolution, and metabolism. *Science* 306:79–86. DOI: 10.1126/science.1101156.

Axtell MJ., Westholm JO., Lai EC. 2011. Vive la différence: biogenesis and evolution of microRNAs in plants and animals. *Genome Biology* 12:221. DOI: 10.1186/gb-2011-12-4-221.

Bailleul B., Rogato A., de Martino A., Coesel S., Cardol P., Bowler C., Falciatore A., Finazzi G. 2010. An atypical member of the light-harvesting complex stress-related protein family modulates diatom responses to light. *Proceedings of the National Academy of Sciences* 107:18214–18219. DOI: 10.1073/pnas.1007703107/-/DCSupplemental.www.pnas.org/cgi/doi/10.1073/pnas.1007703107.

Berns K., Hijmans EM., Mullenders J., Brummelkamp TR., Velds A., Heimerikx M., Kerkhoven RM., Madiredjo M., Nijkamp W., Weigelt B., Agami R., Ge W., Cavet G., Linsley PS., Beijersbergen RL., Bernards R. 2004. A large-scale RNAi screen in human cells identifies new components of the p53 pathway. *Nature* 428:431–437. DOI: 10.1038/nature02371.

Borchert GM., Lanier W., Davidson BL. 2006. RNA polymerase III transcribes human microRNAs. *Nature Structural & Molecular Biology* 13:1097–1101. DOI: 10.1038/nsmb1167.

Bowler C., Allen AE., Badger JH., Grimwood J., Jabbari K., Kuo A., Maheswari U., Martens C., Maumus F., Otillar RP., Rayko E., Salamov A., Vandepoele K., Beszteri B., Gruber A., Heijde M., Katinka M., Mock T., Valentin K., Verret F., Berges J a., Brownlee C., Cadoret J-P., Chiovitti A., Choi CJ., Coesel S., De Martino A., Detter JC., Durkin C., Falciatore A., Fournet J., Haruta M., Huysman MJJ., Jenkins BD., Jiroutova K., Jorgensen RE., Joubert Y., Kaplan A., Kröger N., Kroth PG., La Roche J., Lindquist E., Lommer M., Martin-Jézéquel V., Lopez PJ., Lucas S., Mangogna M., McGinnis K., Medlin LK., Montsant A., Oudot-Le Secq M-P., Napoli C., Obornik M., Parker MS., Petit J-L., Porcel BM., Poulsen N., Robison M., Rychlewski L., Rynearson T a., Schmutz J., Shapiro H., Siaut M., Stanley M., Sussman MR., Taylor AR., Vardi A., von Dassow P., Vyverman W., Willis A., Wyrwicz LS., Rokhsar DS., Weissenbach J., Armbrust EV., Green BR., Van de Peer Y., Grigoriev I V. 2008. The Phaeodactylum genome reveals the evolutionary history of diatom genomes. *Nature* 456:239–44. DOI: 10.1038/nature07410.

Bozarth A., Maier U-G., Zauner S. 2009. Diatoms in biotechnology: modern tools and applications. *Applied microbiology and biotechnology* 82:195–201. DOI: 10.1007/s00253-008-1804-8.

Chen PY., Wang CK., Soong SC., To KY. 2003. Complete sequence of the binary vector pBI121 and its application in cloning T-DNA insertion from transgenic plants. *Molecular Breeding* 11:287–293. DOI: 10.1023/A:1023475710642.

Daboussi F., Leduc S., Maréchal A., Dubois G., Guyot V., Perez-Michaut C., Amato A.,

PeerJ Preprints | https://doi.org/10.7287/peerj.preprints.2907v1 | CC BY 4.0 Open Access | rec: 4 Apr 2017, publ: 4 Apr 2017

Falciatore A., Juillerat A., Beurdeley M., Voytas DF., Cavarec L., Duchateau P. 2014. Genome engineering empowers the diatom Phaeodactylum tricornutum for biotechnology. *Nature communications* 5:3831. DOI: 10.1038/ncomms4831.

Diner RE., Bielinski VA., Dupont C., Allen AE., Weyman PD. 2016a. Refinement of the Diatom Episome Maintenance Sequence and Improvement of Conjugation-based DNA Delivery Methods. *Frontiers in Bioengineering and Biotechnology* 4:65. DOI: 10.3389/FBIOE.2016.00065.

Diner RE., Noddings CM., Lian NC., Kang AK., McQuaid JB., Jablanovic J., Espinoza JL., Nguyen NA., Anzelmatti MA., Jansson J., Bielinski VA., Karas BJ., Dupont CL., Allen AE., Weyman PD. 2016b. Diatom Centromeres Suggest a Novel Mechanism for Nuclear Gene Acquisition. *bioRxiv*.

Engler C., Kandzia R., Marillonnet S. 2008. A one pot, one step, precision cloning method with high throughput capability. *PLoS ONE* 3. DOI: 10.1371/journal.pone.0003647.

Fuda NJ., Ardehali MB., Lis JT. 2009. Defining mechanisms that regulate RNA polymerase II transcription in vivo. *Nature* 461:186–192. DOI: 10.1038/nature08449.

Hildebrand M., Davis AK., Smith SR., Traller JC., Abbriano R. 2012. The place of diatoms in the biofuels industry. *Biofuels* 3:221–240. DOI: 10.4155/bfs.11.157.

Kamath RS., Fraser AG., Dong Y., Poulin G., Durbin R., Gotta M., Kanapin A., Le Bot N., Moreno S., Sohrmann M., Welchman DP., Zipperlen P., Ahringer J. 2003. Systematic functional analysis of the Caenorhabditis elegans genome using RNAi. *Nature* 421:231–7. DOI: 10.1038/nature01278.

Karas BJ., Diner RE., Lefebvre SC., McQuaid J., Phillips APR., Noddings CM., Brunson JK., Valas RE., Deerinck TJ., Jablanovic J., Gillard JTF., Beeri K., Ellisman MH., Glass JI., Hutchison III C a., Smith HO., Venter JC., Allen AE., Dupont CL., Weyman PD. 2015. Designer diatom episomes delivered by bacterial conjugation. *Nature Communications* 6:6925. DOI: 10.1038/ncomms7925.

Lee Y., Kim M., Han J., Yeom K-H., Lee S., Baek SH., Kim VN. 2004. MicroRNA genes are transcribed by RNA polymerase II. *Embo J* 23:4051–4060. DOI: 10.1038/sj.emboj.7600385.

Mock T., Otillar RP., Strauss J., McMullan M., Paajanen P., Schmutz J., Salamov A., Sanges R., Toseland A., Ward BJ., Allen AE., Dupont CL., Frickenhaus S., Maumus F., Veluchamy A., Wu T., Barry KW., Falciatore A., Ferrante MI., Fortunato AE., Glöckner G., Gruber A., Hipkin R., Janech MG., Kroth PG., Leese F., Lindquist EA., Lyon BR., Martin J., Mayer C., Parker M., Quesneville H., Raymond JA., Uhlig C., Valas RE., Valentin KU., Worden AZ., Armbrust EV., Clark MD., Bowler C., Green BR., Moulton V., van Oosterhout C., Grigoriev I V. 2017. Evolutionary genomics of the cold-adapted diatom Fragilariopsis cylindrus. *Nature*. DOI: 10.1038/nature20803.

Nelson D., Tréguer P., Brzezinski M., Leynaert A., Queguiner B. 1995. Production and dissolution of biogenic silica in the ocean: revised global estimates, comparison with regional data and relationship to biogenic sedimentation. *Global Biogeochemical Cycle* 9:359–372.

Nymark M., Sharma AK., Sparstad T., Bones AM., Winge P. 2016. A CRISPR/Cas9 system adapted for gene editing in marine algae. *Scientific reports* 6:24951. DOI: 10.1038/srep24951.

De Riso V., Raniello R., Maumus F., Rogato A., Bowler C., Falciatore A. 2009. Gene silencing in the marine diatom Phaeodactylum tricornutum. *Nucl. Acids Res.* 37:e96. DOI:

PeerJ Preprints | https://doi.org/10.7287/peerj.preprints.2907v1 | CC BY 4.0 Open Access | rec: 4 Apr 2017, publ: 4 Apr 2017

10.1093/nar/gkp448.

Siaut M., Heijde M., Mangogna M., Montsant A., Coesel S., Allen A., Manfredonia A., Falciatore A., Bowler C. 2007. Molecular toolbox for studying diatom biology in Phaeodactylum tricornutum. *Gene* 406:23–35. DOI: 10.1016/j.gene.2007.05.022.

Strack RL., Disney MD., Jaffrey SR. 2013. A superfolding Spinach2 reveals the dynamic nature of trinucleotide repeat RNA. *Nature Methods* 10:1219–1224. DOI: 10.1038/nmeth.2701.

Trentacoste EM., Shrestha RP., Smith SR., Glé C., Hartmann AC., Hildebrand M., Gerwick WH. 2013. Metabolic engineering of lipid catabolism increases microalgal lipid accumulation without compromising growth. *Proceedings of the National Academy of Sciences of the United States of America*. DOI: 10.1073/pnas.1309299110.

Turowski TW., Tollervey D. 2016. Transcription by RNA polymerase III: insights into mechanism and regulation. *Biochemical Society Transactions* 44:1367–1375. DOI: 10.1042/BST20160062.

Wang L., Zheng J., Luo Y., Xu T., Zhang Q., Zhang L., Xu M., Wan J., Wang MB., Zhang C., Fan Y. 2013. Construction of a genomewide RNAi mutant library in rice. *Plant Biotechnology Journal* 11:997–1005. DOI: 10.1111/pbi.12093.

Weyman PD., Beeri K., Lefebvre SC., Rivera J., Mccarthy JK., Heuberger AL., Peers G., Allen AE., Dupont CL. 2015. Inactivation of Phaeodactylum tricornutum urease gene using transcription activator-like effector nuclease-based targeted mutagenesis. *Plant biotechnology journal* 13:460–470. DOI: 10.1111/pbi.12254.

PeerJ Preprints | https://doi.org/10.7287/peerj.preprints.2907v1 | CC BY 4.0 Open Access | rec: 4 Apr 2017, publ: 4 Apr 2017

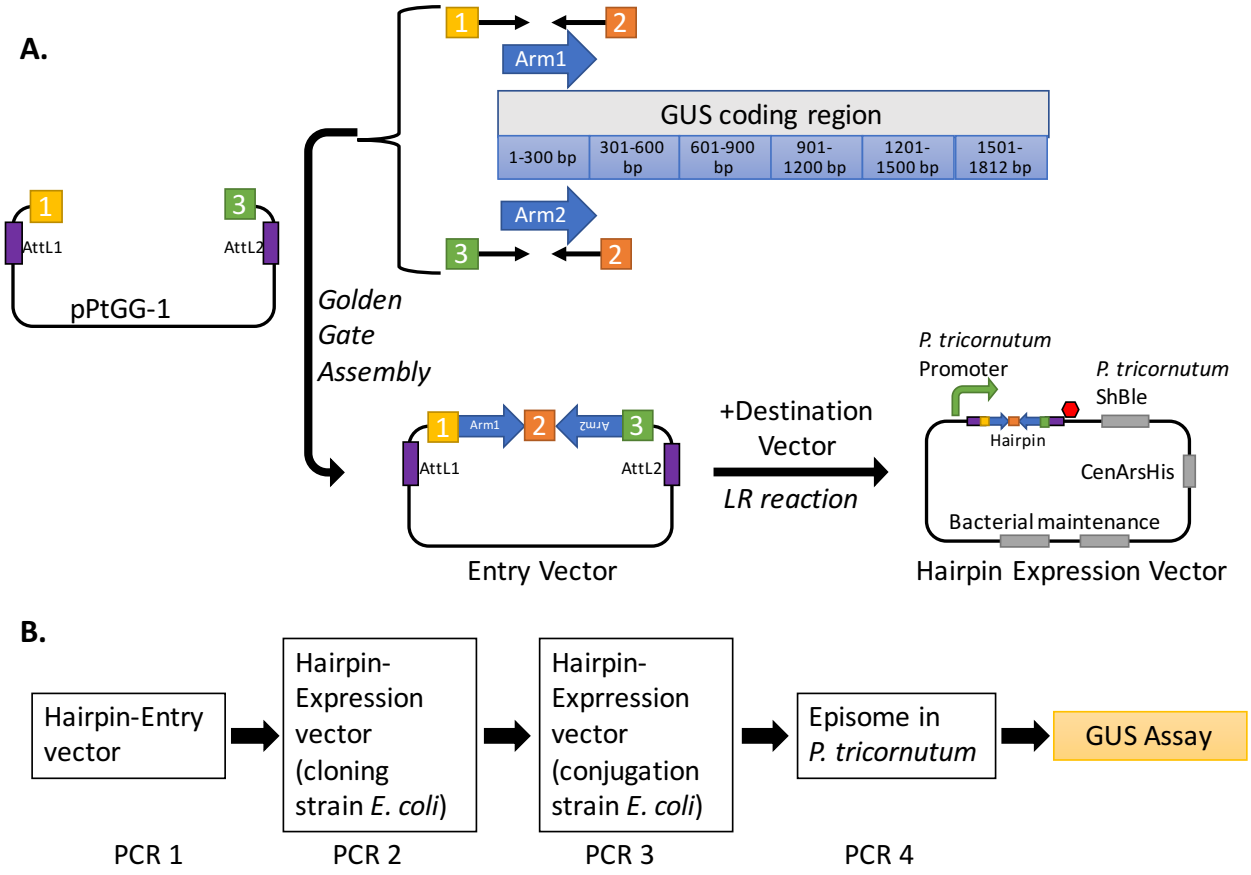

Figure 1: Construction and testing of hairpin expression plasmids. **A.** Regions of the target gene (e.g. *GUS* in this example) were amplified using primers containing adapter sequences for Golden Gate assembly. The numbers (e.g. yellow "1", orange "2", and green "3") indicate unique 4-nt overhangs created during Golden Gate that allow for the correct order of assembly. Entry vectors containing hairpins were then recombined into destination vectors using the LR reaction (Invitrogen) to create hairpin expression vectors. **B.** Screening protocol for hairpin maintenance before GUS assay. PCRs were performed to verify the presence of both arms of the hairpin after each transfer of the hairpin to a new vector or cell line.

PeerJ Preprints | https://doi.org/10.7287/peerj.preprints.2907v1 | CC BY 4.0 Open Access | rec: 4 Apr 2017, publ: 4 Apr 2017

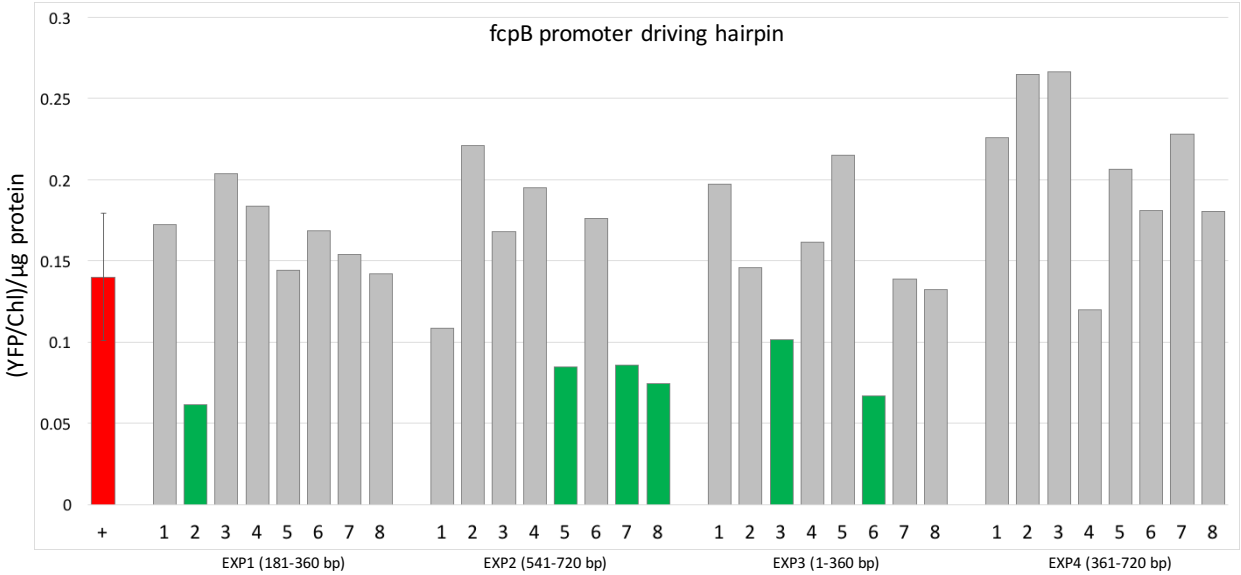

675

Figure 2: Knockdown of YFP expression from four different hairpin constructs (Exp-1 through Exp-4). Eight *P. tricornutum* lines were tested for each construct. The coordinates of the YFP coding region targeted by the hairpin are indicated in parentheses for each construct. The
680 reported value is the YFP fluorescence from which background chlorophyll-A fluorescence was subtracted and this value was then normalized to OD750. The empty vector control treatment ("+") is plotted as the mean value of 8 lines with error bars indicating one standard deviation of the mean. Hairpin-expressing lines with YFP values lower than the confidence interval of one standard deviation are shown in green.

685

PeerJ Preprints | https://doi.org/10.7287/peerj.preprints.2907v1 | CC BY 4.0 Open Access | rec: 4 Apr 2017, publ: 4 Apr 2017

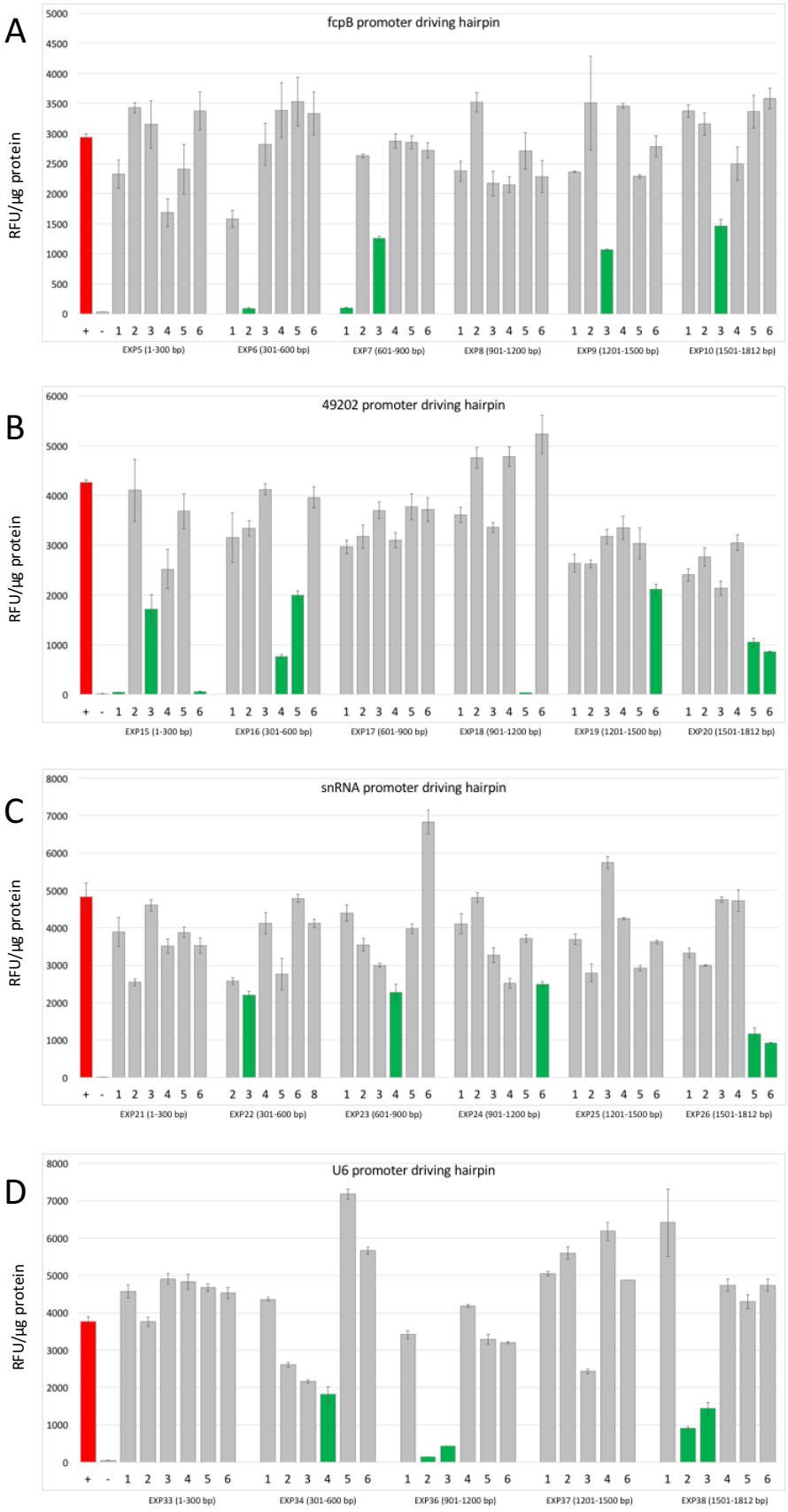

PeerJ Preprints | https://doi.org/10.7287/peerj.preprints.2907v1 | CC BY 4.0 Open Access | rec: 4 Apr 2017, publ: 4 Apr 2017

Figure 3: (previous page) Knockdown of GUS expression by 6 different hairpin constructs. The 6 hairpin constructs were driven by the different promoters: FcpB (A), 49202 (B), snRNA (C), and U6 (D). Note that data for EXP35 (U6 driven hairpin at positions 601-900-bp) is missing due to difficulties conjugating this construct into *P. tricornutum*. The parental GUS-expressing reporter strain ("+") and non-expressing GUS control ("-") are included for each promoter. Error bars indicate one standard deviation of the mean for three technical replicates. Lines with knockdown of 50% or greater compared to the parental line are shown in green.

PeerJ Preprints | https://doi.org/10.7287/peerj.preprints.2907v1 | CC BY 4.0 Open Access | rec: 4 Apr 2017, publ: 4 Apr 2017

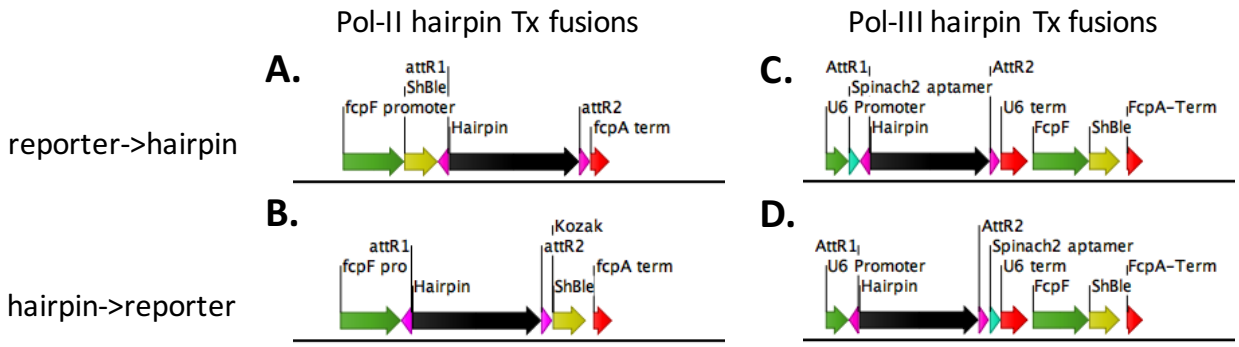

700

Figure 4: Maps showing vectors designed to express hairpins as transcriptional fusions. FcpB-driven fusions between the hairpin and the ShBle transcript were designed such that the ShBle resistance gene was expressed before (A) or after (B) the hairpin on the transcript. Similarly, for the U6 promoter, fusions with the fluorescent spinach aptamer were constructed with the hairpin
705 expressed before (C) or after (D) the aptamer reporter.

PeerJ Preprints | https://doi.org/10.7287/peerj.preprints.2907v1 | CC BY 4.0 Open Access | rec: 4 Apr 2017, publ: 4 Apr 2017

710 **Table 1: Primers and plasmid/strain names of YFP-targeted hairpins**

YFP region targeted	Primers to amplify region to make entry vector	FcpB hairpin expression plasmid (resulting *P. tricornutum* line)
1-200 bp	Left arm: YFP-RNAi-21+YFP-RNAi-22 Right arm: YFP-RNAi-23+YFP-RNAi-24	Exp-1
181-360 bp	Left arm: YFP-RNAi-25 +YFP-RNAi-26 Right arm: YFP-RNAi-27+YFP-RNAi-28	Exp-2
1-360 bp	Left arm: YFP-RNAi-37 +YFP-RNAi-38 Right arm: YFP-RNAi-39 +YFP-RNAi-40	Exp-3
361-720 bp	Left arm: YFP-RNAi-41 +YFP-RNAi-42 Right arm: YFP-RNAi-43+YFP-RNAi-44	Exp-4

PeerJ Preprints | https://doi.org/10.7287/peerj.preprints.2907v1 | CC BY 4.0 Open Access | rec: 4 Apr 2017, publ: 4 Apr 2017

715 **Table 2: Primers and plasmid/strain names of GUS-targeted hairpins**

GUS region targeted	Primers to amplify region to make entry vector	FcpB expression of hairpin (Resulting *P. tricornutum* line)	49202 expression of hairpin (Resulting *P. tricornutum* line)	U6 expression of hairpin (Resulting *P. tricornutum* line)	snRNA expression of hairpin (Resulting *P. tricornutum* line)
1-300 bp	Left arm: GUS-RNAi-13 +GUS-RNAi-14 Right arm: GUS-RNAi-15+GUS-RNAi-16	Exp-6	Exp-15	Exp-33	Exp-21
301-600 bp	Left arm: GUS-RNAi-17+GUS-RNAi-18 Right arm: GUS-RNAi-19+GUS-RNAi-20	Exp-7	Exp-16	Exp-34	Exp-22
601-900 bp	Left arm: GUS-RNAi-21+GUS-RNAi-22 Right arm: GUS-RNAi-23+GUS-RNAi-24	Exp-8	Expi-17	No colonies recovered (Exp-35)	Exp-23
901-1200 bp	Left arm: GUS-RNAi-25+GUS-RNAi-26 Right arm: GUS-RNAi-27+GUS-RNAi-28	Exp-9	Exp-18	Exp-36	Exp-24
1201-1500 bp	Left arm: GUS-RNAi-29+GUS-RNAi-30 Right arm: GUS-RNAi-31+GUS-RNAi-32	Exp-5	Exp-19	Exp-37	Exp-25
1501-1812 bp	Left arm: GUS-RNAi-33+GUS-RNAi-34 Right arm: GUS-RNAi-35+GUS-RNAi-36	Exp-10	Exp-20	Exp-38	Exp-26

PeerJ Preprints | https://doi.org/10.7287/peerj.preprints.2907v1 | CC BY 4.0 Open Access | rec: 4 Apr 2017, publ: 4 Apr 2017

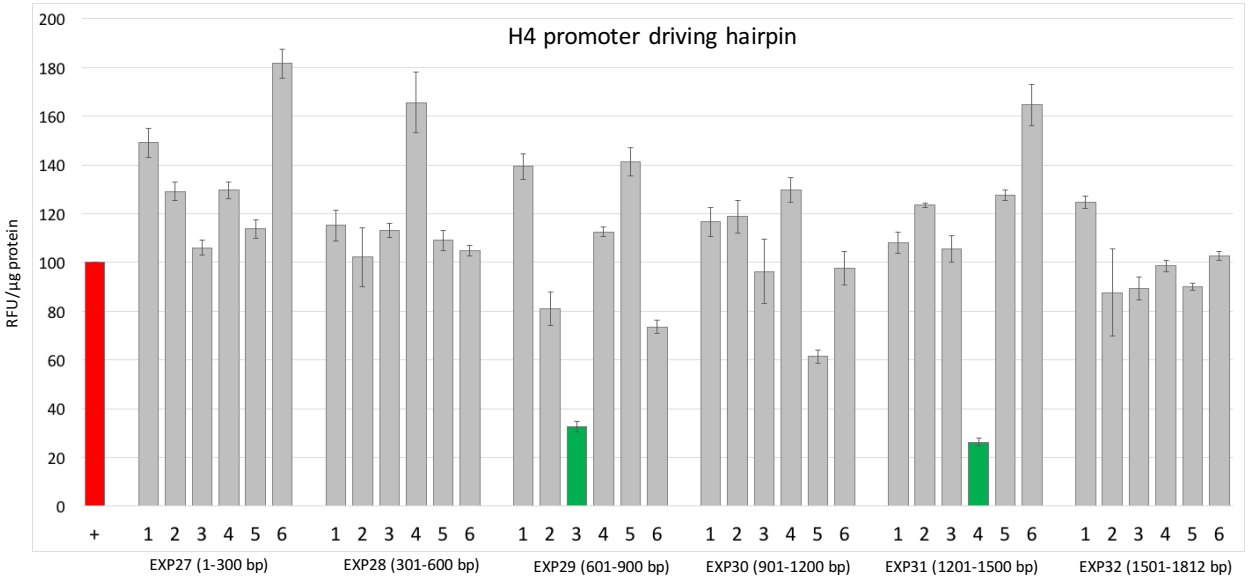

Supplemental Figure 1: Knockdown of GUS expression by 6 different hairpin constructs driven by H4 Promoter. Each of the six 300-bp hairpins were driven by the H4 promoter. Due to differences in the absolute value of the samples that were assayed on different days, GUS expression is given as a percent of the parental GUS-expressing strain (assays performed on different days each had their own GUS-expressing control to allow the experiments to be compared). Error bars indicate one standard deviation of the mean for three technical replicates.

PeerJ Preprints | https://doi.org/10.7287/peerj.preprints.2907v1 | CC BY 4.0 Open Access | rec: 4 Apr 2017, publ: 4 Apr 2017

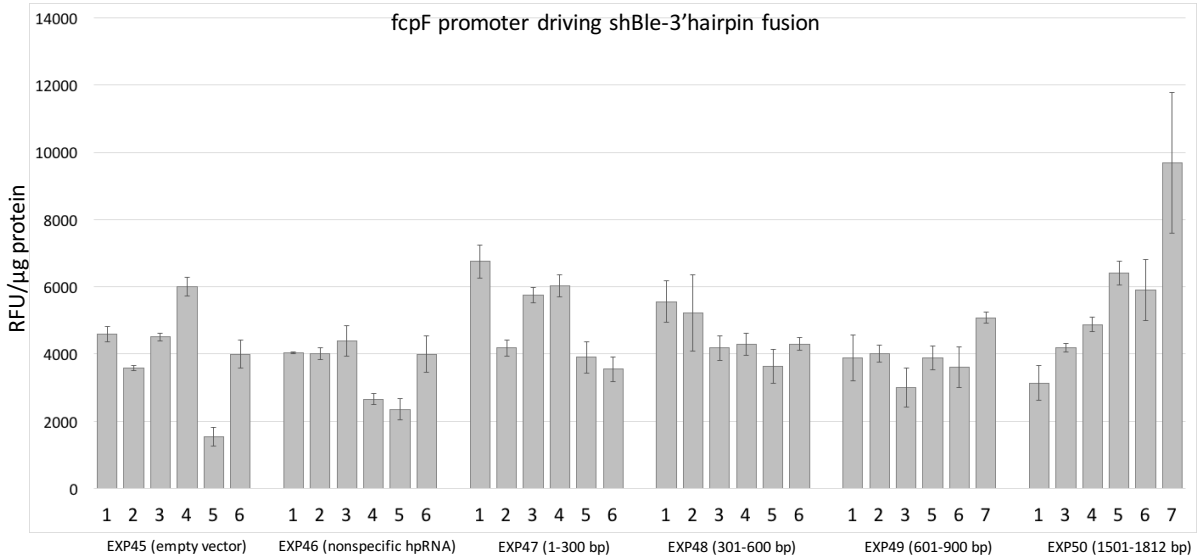

730

Supplemental Figure 2: Knockdown of GUS expression using ShBle-hairpin transcriptional fusions. Error bars indicate one standard deviation of the mean for three technical replicates.

735

PeerJ Preprints | https://doi.org/10.7287/peerj.preprints.2907v1 | CC BY 4.0 Open Access | rec: 4 Apr 2017, publ: 4 Apr 2017

Supplemental Table 1: Primers used in this study

Primer name	Primer Sequence (5'-)
F-OH	GCGCAACGTTGTTGCCATTGTCCCAGTCACGACGTTGTAAAACGAC
Riceintron1	GGTACGTTTACATGTTTTTTTTCCCTTCATATCGATTTTTTTTTGGCGCAG
R-OH	AATGTTGCAGCACTGACCCTTCACTATAGGGGATATCAGCTGGATGG
Riceintron2	CTGCGCCAAAAAAAAATCGATATGAAGGGAAAAAAAACATGTAAACGTACC
Ptrnai-47	CAGGGTTTTCCCAGTCACGACGTTGTAAAACGACGGCCAGTGGCAATCTCACGCACCAGG
Ptrnai-48	gtgatatcaagcttatcgataccgtcgacttgacttGTTGGCTGTTGTTTGTTTTCGGTA
Ptrnai-49	CACTGGCCGTCGTTTTACAAC
Ptrnai-50	CGTTCATCCATAGTTGCCTGA
Ptrnai-51	TCTCGCGGTATCATTGCAGC
Ptrnai-52.2	aagtcaagtcgacggtatcgataagcttgatatcacaagtttgtacaaaaaagctgaacg
Ptrnai-53	CAGGGTTTTCCCAGTCACGACGTTGTAAAACGACGGCCAGTGATCGCACCCGTCCAAACG
Ptrnai-54	aaacttgtgatatcaagcttatcgataccgtcgacttgacttGGTGGTGCGGAAAGAGGC
Ptrnai-31	tgaataggcgagattccgcggtggagctccaattcgccctATCTTCCGCTGCATAACCCT
Ptrnai-32	TTGGTTTCACAGTCAGGAATAACACTAGCTCGTCTTCAacGGCCATTCGCCATTCAGGCT
Ptrnai-29	GCTATAATGACCCCGAAGCAGGGTTATGCAGCGGAAGATagggcgaattggagctccacc
Ptrnai-22	CCTCACTGAAAGTGTCCCAGCCAAAGTCGAGGTAGttacttgtacagctcgtccatgccg
Ptrnai-23	cgccgggatcactctcggcatggacgagctgtacaagtaaCTACCTCGACTTTGGCTGGG
Ptrnai-30	CCAACAGTTGCGCAGCCTGAATGGCGAATGGCCgtTGAAGACGAGCTAGTGTTATTCCTG

PeerJ Preprints | https://doi.org/10.7287/peerj.preprints.2907v1 | CC BY 4.0 Open Access | rec: 4 Apr 2017, publ: 4 Apr 2017

BackR	TAAGCCGTGTCGTCAAGAGTGGTCATGGGTACCCTCAGCTAGAATATTA
PtRNAi-7	AAGTCGACGGTATCGATAATATTCTAGCTGAGGGTACCCATGACCACTCTTGACGACACG
BackF	TCTACATGAGCATGCCCTGCCCCTGACCGACGCCGACCAACACCGCC
PtRNAi-8	CCGTCGGGCCGCGTCGGACCGGCGGTGTTGGTCGGCGTCGGTCAGGGGCAGGGCATGCTC
PtRNAi-25	TTTGATTTCACGGGTTGGGGTTTCTACAGGACGTAACATGGTGAAGGGGGCGGCCGCGGA
PtRNAi-29	GCTATAATGACCCCGAAGCAGGGTTATGCAGCGGAAGATagggcgaattggagctccacc
PtRNAi-31	tgaataggcgagattccgcggtggagctccaattcgccctATCTTCCGCTGCATAACCCT
PBR-nanoluc5	TCATGTTTGACAGCTTATCATCG
PtRNAi-26	TACAAAAAAGCAGGCTCCGCGGCCGCCCCCTTCACCATGTTACGTCCTGTAGAAACCCCA
PtRNAi-27	TGTCCTCACTGAAAGTGTCCCAGCCAAAGTCGAGGTAGTCATTGTTTGCCTCCCTGCTGC
PtRNAi-28	GAACTTCGGTGAAAAACCGCAGCAGGGAGGCAAACAATGACTACCTCGACTTTGGCTGGG
PtRNAi-30	CCAACAGTTGCGCAGCCTGAATGGCGAATGGCCgtTGAAGACGAGCTAGTGTTATTCCTG
PtRNAi-32	TTGGTTTCACAGTCAGGAATAACACTAGCTCGTCTTCAacGGCCATTCGCCATTCAGGCT
PBR-nanoluc4	TGCCTGACTGCGTTAGCAA
Ptrnai-3	TTCCCAGTCACGACGTTGTAAAACGACGGCCAGTGaatctcgcctattcatggtgtatac
Ptrnai-4	GTGAGGGTTAATTTCGAGCTTGGCGTAATCATGGTcctgaagacgagctagtgttattcc
Ptrnai-5	ttggtttcacagtcaggaataacactagctcgtcttcaggACCATGATTACGCCAAGCTC
Ptrnai-6	tggatgttgaacttgtatacaccatgaataggcgagattCACTGGCCGTCGTTTTACAAC

PeerJ Preprints | https://doi.org/10.7287/peerj.preprints.2907v1 | CC BY 4.0 Open Access | rec: 4 Apr 2017, publ: 4 Apr 2017

GUS-RNAi-13	atcgaGGTCTCaATGGATGTTACGTCCTGTAGAAACCCCAACC
GUS-RNAi-14	GAGCTGGTCTCACTTCATATCGATTTTTTTTTGGCGCAGATTGACCCAC ACTTTGCCGTAATGAGTGA
GUS-RNAi-15	tgcacGGTCTCaGAAGGGAAAAAAAACATGTAAACGTACCATTGACCCAC ACTTTGCCGTAATGAGT
GUS-RNAi-16	TGAGCGGTCTCTAGGTATGTTACGTCCTGTAGAAACCCCAACC
GUS-RNAi-17	atcgaGGTCTCaATGGAATCAGGAAGTGATGGAGCATCAGGG
GUS-RNAi-18	GAGCTGGTCTCACTTCATATCGATTTTTTTTTGGCGCAGCGCGTGGTTA CAGTCTTGCGCG
GUS-RNAi-19	tgcacGGTCTCaGAAGGGAAAAAAAACATGTAAACGTACCCGCGTGGTTA CAGTCTTGCGCG
GUS-RNAi-20	TGAGCGGTCTCTAGGTAATCAGGAAGTGATGGAGCATCAGGG
GUS-RNAi-21	atcgaGGTCTCaATGGTCTGTTGACTGGCAGGTGGTGG
GUS-RNAi-22	GAGCTGGTCTCACTTCATATCGATTTTTTTTTGGCGCAGGTCCGCATCT TCATGACGACCAAAG
GUS-RNAi-23	tgcacGGTCTCaGAAGGGAAAAAAAACATGTAAACGTACCGTCCGCATCT TCATGACGACCAAAG
GUS-RNAi-24	TGAGCGGTCTCTAGGTTCTGTTGACTGGCAGGTGGTGG
GUS-RNAi-25	atcgaGGTCTCaATGGTTGCGTGGCAAAGGATTCGATAACGTG
GUS-RNAi-26	GAGCTGGTCTCACTTCATATCGATTTTTTTTTGGCGCAGTTTGTCACGC GCTATCAGCTCTTTAATCG
GUS-RNAi-27	tgcacGGTCTCaGAAGGGAAAAAAAACATGTAAACGTACCTTTGTCACGC GCTATCAGCTCTTTAATCG
GUS-RNAi-28	TGAGCGGTCTCTAGGTTTGCGTGGCAAAGGATTCGATAACGTG
GUS-RNAi-29	atcgaGGTCTCaATGGAACCACCCAAGCGTGGTGATGTG
GUS-RNAi-30	GAGCTGGTCTCACTTCATATCGATTTTTTTTTGGCGCAGAATCGGCTGA TGCAGTTTCTCCTGC
GUS-RNAi-31	tgcacGGTCTCaGAAGGGAAAAAAAACATGTAAACGTACCAATCGGCTGA TGCAGTTTCTCCTGC

PeerJ Preprints | https://doi.org/10.7287/peerj.preprints.2907v1 | CC BY 4.0 Open Access | rec: 4 Apr 2017, publ: 4 Apr 2017

GUS-RNAi-32	TGAGCGGTCTCTAGGTAACCACCCAAGCGTGGTGATGTG
GUS-RNAi-33	atcgaGGTCTCaATGGATCATCACCGAATACGGCGTGGATAC
GUS-RNAi-34	GAGCTGGTCTCACTTCATATCGATTTTTTTTTGGCGCAGTCATTGTTTG CCTCCCTGCTGCG
GUS-RNAi-35	tgcacGGTCTCaGAAGGGAAAAAAAACATGTAAACGTACCTCATTGTTTG CCTCCCTGCTGCG
GUS-RNAi-36	TGAGCGGTCTCTAGGTATCATCACCGAATACGGCGTGGATAC
5'hpRNA-F-OH	GCGCAACGTTGTTGCCATTGTCCCAGTCACGACGTTGTAAAACGAC
3'hpRNA-R-OH	AATGTTGCAGCACTGACCCTTCACTATAGGGGATATCAGCTGGATGG
5'hpRNA-F-vector	AGGGTCAGTGCTGCAACATTATCACGAGGCCCTTTCGTCTTCAAG
3'hpRNA-R-vector	CAATGGCAACAACGTTGCGCCTTAACGTGAGTTTTCGTTCCACTGAGC
PtRNAi-43	cagtcGGTCTCaACCTGCGGCCGCACCCAGCTTTCTTGTACAAAGTTGGC ATTATAAG
PtRNAi-44	tgagtGGTCTCaCCATGCGGCCGCAGCCTGCTTTTTTGTACAAAGTTGGC ATTATAAAAAAG
snRNAI-DEST-BB-F	TTGCAGAAAATCATAGTTTTacaagtttgtacaaaaaagctgaacgagaaacgtaa
snRNAI-DEST-BB-R	CACTGGCCGTCGTTTTACAACGTCGT
snRNAiPro-F	TTGTAAAACGACGGCCAGTGCTTCTGCAGCTCTTCCAAATCGTACA
snRNAiPro-R	AAAACTATGATTTTCTGCAAATATATAAATAGAAAGAGTATACCTATACA CAATAACTG
snRNAiterm-F	acaaagtggtgaattctgagTTTTGCCTTTTGACCGAAAGCTATCTTACTTACTAC
snRNAiterm-R	GAGCTTGGCGTAATCATGGTTCGAGCAGTTCTAGAAGAAGTGTTTATCT TTACC
Backbone 33	TCTCATGTTTGACAGCTTATCATCGATAAGC
DEST-cas-R	AAAGGCAAAActcagaattcaccactttgtacaagaaagctgaacgagaaac

PeerJ Preprints | https://doi.org/10.7287/peerj.preprints.2907v1 | CC BY 4.0 Open Access | rec: 4 Apr 2017, publ: 4 Apr 2017

Backbone 34	CTTCTTCTAGAACTGCTCGAACCATGATTACGCCAAGCTCGAAATTAACC
Backbone 35	TGCCTGACTGCGTTAGCAATTTAACTGTGATAAA
Backbone 36	TCTCATGTTTGACAGCTTATCATCGATAAGCTTTAATGCGG
U6 term-F	acaaagtggtgaattctgagAGAACCGCTCACCCATGCTATCGTAT
U6 term-R	GAGCTTGGCGTAATCATGGTGCAGAAAAGTTCGTCGAGACCATGG
U6-DEST-cas-F	AAAACACCTTCAAAGTCGAGacaagtttgtacaaaaaagctgaacgagaaacgtaa
U6-DEST-cas-R	TAGCATGGGTGAGCGGTTCTctcagaattcaccactttgtacaagaaagctg
Backbone-shble-F	GTCTCGACGAACTTTTCTGCACCATGATTACGCCAAGCTCGAAATTAACC
Backbone 37-R	TGCCTGACTGCGTTAGCAATTTAACTGTGATAAA
Backbone 38-F	TCTCATGTTTGACAGCTTATCATCGATAAGCTTTAATGCGG
U6-Backbone 39-R	ACACCAACTTCCGAGCCAACCACTGGCCGTCGTTTTACAACGTCGT
U6-Pro-F	TTGTAAAACGACGGCCAGTGGTTGGCTCGGAAGTTGGTGTTGAC
U6-Pro-R	gctttttttgtacaaacttgtCTCGACTTTGAAGGTGTTTTTTGACCTTATAAAGC
Backbone 40-R	gctttttttgtacaaacttgtTCAGTCCTGCTCCTCGGC
shBle-3'fusion-DESTcasF	TGGCCGAGGAGCAGGACTGAacaagtttgtacaaaaaagctgaacgagaaacgtaa
shBle-3'fusion-DESTcasR	CCCAGCCAAAGTCGAGGTAGaccactttgtacaagaaagctgaacgagaaac
fcpA term-F	gctttcttgtacaaagtggtCTACCTCGACTTTGGCTGGGACA
shBle-F	gctttcttgtacaaagtggtGCCACCATGGCCAAGTTGACCAGTGCC
fcpF pro-R	gctttttttgtacaaacttgtGGGTACCCTCAGCTAGAATATTATCGATACCGTC
5'fusion-shBle-DESTcasF	TATTCTAGCTGAGGGTACCCacaagtttgtacaaaaaagctgaacgagaaacgtaa
5'fusion-shBle-DESTcasR	ACTTGGCCATGGTGGCaccactttgtacaagaaagctgaacgagaaac

PeerJ Preprints | https://doi.org/10.7287/peerj.preprints.2907v1 | CC BY 4.0 Open Access | rec: 4 Apr 2017, publ: 4 Apr 2017

U6 Pro-R-5'Spinach	AGCCTGCTTTTTTGTACAAACTCGACTTTGAAGGTGTTTTTTGACCTTATAAAGC
U6-5'-Spinach-F	AAAACACCTTCAAAGTCGAGTTTGTACAAAAAAGCAGGCTGATGTAACTGAATGAAATGGTG
U6-5'-Spinach-R	gctttttttgtacaaacttgtTTTGTACAAGAAAGCTGGGTGATGTAACTAGTTACGGA
U6-5'Spinach-DESTcasF	ACCCAGCTTTCTTGTACAAAacaagtttgtacaaaaaagctgaacgagaaacgtaa
U6-DEST-3'Sp-cas-R	AGCCTGCTTTTTTGTACAAActcagaattcaccactttgtacaagaaagctg
U6-3'-Spinach-F	acaaagtggtgaattctgagTTTGTACAAAAAAGCAGGCTGATGTAACTGAATGAAATGGTG
U6-3'-Spinach-R	TAGCATGGGTGAGCGGTTCTTTTGTACAAGAAAGCTGGGTGATGTAACTAGTTACGGA
U6 term-F-noOH	AGAACCGCTCACCCATGCTATCGTAT
PtGG-1 “MCS” Ultramer F	TGGGAATTCGTTAACAGATCTGaGaCCGCGGCTCGAGACTAGTGCCTAGGTGAGTTTCTATTCGCAGTCGGCTGATCTGTGTGAAAtagggataacagggtaatTCTTAATGAAGGGTCCAATTACCAATTTGAAACTCAGCTAGCTCTAGAATATCAATTGGGATCCggtctcatcgacaAAGGGTGGGCGCGCCG
PtGG-1 “MCS” Ultramer R	CGGCGCGCCCACCCTTtgtcgatgagaccGGATCCCAATTGATATTCTAGAGCTAGCTGAGTTTCAAATTGGTAATTGGACCCTTCATTAAGAattaccctgttatcctaTTTCACACAGATCAGCCGACTGCGAATAGAAACTCACCTAGGCACTAGTCTCGAGCCGCGGtCtCAGATCTGTTAACGAATTCCCAggtgAAGGGGGCGGCCGCGG
Spinach2-sense Ultramer	TTTGTACAAAAAAGCAGGCTGATGTAACTGAATGAAATGGTGAAGGACGGGTCCAGTAGGCTGCTTCGGCAGCCTACTTGTTGAGTAGAGTGTGAGCTCCGTAACTAGTTACATCACCCAGCTTTCTTGTACAAA
Spinach2-antisense Ultramer	TTTGTACAAGAAAGCTGGGTGATGTAACTAGTTACGGAGCTCACACTCTACTCAACAAGTAGGCTGCCGAAGCAGCCTACTGGACCCGTCCTTCACCATTTCATTCAGTTACATCAGCCTGCTTTTTTGTACAAA
YFP-RNAi-21	atcgaGGTCTCaATGGatggtgagcaagggcgaggagct
YFP-RNAi-22	GAGCTGGTCTCACTTCATATCGATTTTTTTTTGGCGCAGtgcaggccgtagccgaaggtgg

PeerJ Preprints | https://doi.org/10.7287/peerj.preprints.2907v1 | CC BY 4.0 Open Access | rec: 4 Apr 2017, publ: 4 Apr 2017

YFP-RNAi-23	tgcacGGTCTCaGAAGGGAAAAAAAACATGTAAACGTACCtgcaggccgtagccgaaggtgg
YFP-RNAi-24	TGAGCGGTCTCTAGGTatggtgagcaagggcgaggagct
YFP-RNAi-25	atcgaGGTCTCaATGGctcgtgaccaccttcggctacg
YFP-RNAi-26	GAGCTGGTCTCACTTCATATCGATTTTTTTTTGGCGCAGcagggtgtcgccctcgaacttca
YFP-RNAi-27	tgcacGGTCTCaGAAGGGAAAAAAAACATGTAAACGTACCcagggtgtcgccctcgaacttca
YFP-RNAi-28	TGAGCGGTCTCTAGGTctcgtgaccaccttcggctacg
YFP-RNAi-37	atcgaGGTCTCaATGGatggtgagcaagggcgaggagct
YFP-RNAi-38	GAGCTGGTCTCACTTCATATCGATTTTTTTTTGGCGCAGcagggtgtcgccctcgaacttca
YFP-RNAi-39	tgcacGGTCTCaGAAGGGAAAAAAAACATGTAAACGTACCcagggtgtcgccctcgaacttca
YFP-RNAi-40	TGAGCGGTCTCTAGGTatggtgagcaagggcgaggagct
YFP-RNAi-41	atcgaGGTCTCaATGGgtgaaccgcatcgagctgaagg
YFP-RNAi-42	GAGCTGGTCTCACTTCATATCGATTTTTTTTTGGCGCAGttacttgtacagctcgtccatgccgag
YFP-RNAi-43	tgcacGGTCTCaGAAGGGAAAAAAAACATGTAAACGTACCttacttgtacagctcgtccatgccgag
YFP-RNAi-44	TGAGCGGTCTCTAGGTgtgaaccgcatcgagctgaagg

PeerJ Preprints | https://doi.org/10.7287/peerj.preprints.2907v1 | CC BY 4.0 Open Access | rec: 4 Apr 2017, publ: 4 Apr 2017

Supplementary Table 2: Raw data for all YFP and GUS experiments						
		OD750	CHL	(YFP/CHL)/OD norm		
fcpB YFP	EXP5-1	0.910	0.156	0.171		
	EXP5-2	0.824	0.142	0.172		
	EXP5-3	0.883	0.209	0.237		
	EXP5-4	0.895	0.130	0.145		
	EXP5-5	0.834	0.101	0.121		
	EXP5-6	0.907	0.129	0.142		
	EXP5-7	0.894	0.158	0.177		
	EXP5-8	0.840	0.095	0.113		
	EXP1-1	0.744	0.128	0.172		
	EXP1-2	0.830	0.051	0.061		
	EXP1-3	0.834	0.170	0.204		
	EXP1-4	0.866	0.159	0.184		
	EXP1-5	0.674	0.097	0.144		
	EXP1-6	0.807	0.136	0.169		
	EXP1-7	0.846	0.130	0.154		
	EXP1-8	0.978	0.139	0.142		
	EXP2-1	0.757	0.082	0.108		
	EXP2-2	0.824	0.182	0.221		
	EXP2-3	0.749	0.126	0.168		
	EXP2-4	0.784	0.153	0.195		
	EXP2-5	0.837	0.071	0.085		
	EXP2-6	0.829	0.146	0.176		
	EXP2-7	0.803	0.069	0.086		
	EXP2-8	0.899	0.067	0.075		
	EXP3-1	0.817	0.161	0.197		
	EXP3-2	0.767	0.112	0.146		
	EXP3-3	0.838	0.085	0.101		
	EXP3-4	0.810	0.131	0.162		
	EXP3-5	0.824	0.177	0.215		
	EXP3-6	0.851	0.057	0.067		
	EXP3-7	0.741	0.103	0.139		
	EXP3-8	0.764	0.101	0.132		
	EXP4-1	0.792	0.179	0.226		
	EXP4-2	0.805	0.213	0.265		
	EXP4-3	0.781	0.208	0.266		
	EXP4-4	0.791	0.095	0.120		
	EXP4-5	0.810	0.167	0.206		
	EXP4-6	0.846	0.153	0.181		
	EXP4-7	0.873	0.199	0.228		
	EXP4-8	0.842	0.152	0.181		

		rep 1	**rep 2**	**rep 3**	**average**	**stdev**
fcpB GUS	pos control	3000.056	2880.922	2923.033	2934.670	60.414
	neg control	29.277	28.276	30.585	29.379	1.158
	EXP5-1	2147.891	2231.566	2591.900	2323.786	235.933
	EXP5-2	3496.527	3451.718	3335.573	3427.939	83.070
	EXP5-3	3357.483	3410.573	2695.446	3154.501	398.438
	EXP5-4	1820.147	1805.168	1421.783	1682.366	225.796
	EXP5-5	2825.937	2399.295	2001.892	2409.041	412.109
	EXP5-6	3640.465	3468.755	3031.847	3380.356	313.791
	EXP6-1	1650.309	1666.056	1409.751	1575.372	143.648
	EXP6-2	95.746	93.449	61.774	83.656	18.985
	EXP6-3	2910.888	3111.175	2433.644	2818.569	348.072
	EXP6-4	3475.072	3792.537	2895.650	3387.753	454.775
	EXP6-5	3850.809	3660.912	3075.135	3528.952	404.324
	EXP6-6	3531.307	3546.752	2925.276	3334.445	354.435
	EXP7-1	100.856	94.454	91.124	95.478	4.946
	EXP7-2	2643.466	2594.938	2651.884	2630.096	30.737
	EXP7-3	1272.408	1276.487	1204.873	1251.256	40.221
	EXP7-4	2927.877	2737.370	2949.814	2871.687	116.838
	EXP7-5	2870.442	2957.250	2746.187	2857.960	106.084
	EXP7-6	2580.570	2821.828	2756.895	2719.764	124.841
	EXP8-1	2250.587	2314.791	2565.493	2376.957	166.403
	EXP8-2	3335.010	3595.697	3633.920	3521.542	162.669
	EXP8-3	1938.908	2255.722	2313.822	2169.484	201.787
	EXP8-4	2100.536	2054.654	2293.233	2149.474	126.595
	EXP8-5	2356.144	2890.880	2888.889	2711.971	308.157
	EXP8-6	2419.958	1974.795	2457.109	2283.954	268.383
	EXP9-1	2380.150	2351.150	2359.835	2363.712	14.884
	EXP9-2	3914.888	4002.275	2612.513	3509.892	778.381
	EXP9-3	1075.558	1058.278	1069.121	1067.652	8.733
	EXP9-4	3419.808	3463.218	3499.975	3461.000	40.130
	EXP9-5	2282.988	2320.763	2258.901	2287.551	31.183
	EXP9-6	2623.940	2976.856	2763.832	2788.210	177.717
	EXP10-1	3484.614	3366.408	3278.149	3376.390	103.594
	EXP10-2	3372.733	3029.054	3078.213	3160.000	185.865
	EXP10-3	1479.013	1561.151	1349.928	1463.364	106.478
	EXP10-4	2820.288	2359.156	2312.752	2497.399	280.591
	EXP10-5	3681.501	3203.215	3209.989	3364.902	274.204
	EXP10-6	3757.999	3566.132	3417.213	3580.448	170.843
49202 GUS	pos control	4219.711	4320.274	4235.912	4258.632	53.995
	neg control	13.452	24.648	10.289	16.130	7.545

	EXP15-1	41.882	45.867	48.443	45.397	3.305
	EXP15-2	4312.514	4595.506	3405.774	4104.598	621.520
	EXP15-3	1972.256	1780.378	1396.828	1716.487	292.986
	EXP15-4	2795.942	2703.319	2065.358	2521.540	397.770
	EXP15-5	3286.229	3967.872	3798.651	3684.251	354.929
	EXP15-6	67.387	63.698	53.010	61.365	7.467
	EXP16-1	3255.780	2612.758	3601.429	3156.656	501.734
	EXP16-2	3448.505	3397.707	3163.228	3336.480	152.176
	EXP16-3	4156.458	3999.312	4218.995	4124.922	113.186
	EXP16-4	779.055	715.580	790.924	761.853	40.511
	EXP16-5	1896.986	2007.144	2080.554	1994.895	92.395
	EXP16-6	4072.338	4095.512	3717.035	3961.628	212.141
	EXP17-1	3120.910	2926.258	2854.664	2967.277	137.781
	EXP17-2	3053.671	3029.024	3435.894	3172.863	228.124
	EXP17-3	3834.299	3760.292	3514.188	3702.926	167.589
	EXP17-4	3274.873	2979.672	3053.331	3102.625	153.650
	EXP17-5	3964.992	3878.953	3481.037	3774.994	258.183
	EXP17-6	3834.429	3880.967	3446.084	3720.493	238.782
	EXP18-1	3555.818	3495.400	3783.376	3611.532	151.857
	EXP18-2	4997.315	4671.234	4605.988	4758.179	209.652
	EXP18-3	3335.098	3472.519	3267.738	3358.451	104.369
	EXP18-4	5007.173	4676.800	4654.525	4779.499	197.485
	EXP18-5	36.357	38.466	36.310	37.044	1.232
	EXP18-6	4820.121	5590.986	5281.717	5230.941	387.933
	EXP19-1	2844.615	2566.601	2512.449	2641.222	178.213
	EXP19-2	2553.849	2612.450	2704.401	2623.566	75.889
	EXP19-3	3277.274	3002.278	3241.324	3173.625	149.476
	EXP19-4	3468.221	3499.223	3078.502	3348.648	234.467
	EXP19-5	3217.888	3222.065	2673.198	3037.717	315.690
	EXP19-6	2124.495	2212.669	1999.176	2112.113	107.284
	EXP20-1	2552.165	2316.338	2346.492	2404.998	128.339
	EXP20-2	2549.664	2857.049	2883.698	2763.470	185.640
	EXP20-3	2305.472	2072.838	2041.067	2139.792	144.359
	EXP20-4	2933.865	2989.237	3229.897	3051.000	157.384
	EXP20-5	968.161	1125.953	1059.180	1051.098	79.206
	EXP20-6	870.694	860.835	838.788	856.772	16.336
snRNA GUS	pos control	4883.356	4762.533	4832.682	4826.190	381.436
	neg control	6.500	8.919	6.246	7.220	1.749
	EXP21-1	3617.504	4329.548	3713.947	3887.000	386.279
	EXP21-2	2631.388	2440.130	2557.648	2543.055	96.461
	EXP21-3	4768.379	4568.290	4471.947	4602.872	151.212
	EXP21-4	3694.881	3520.905	3315.080	3510.288	190.123

	EXP21-5	4027.687	3763.154	3834.444	3875.095	136.872
	EXP21-6	3341.653	3511.948	3745.507	3533.036	202.751
	EXP22-2	2652.302	2482.510	2584.216	2573.009	85.449
	EXP22-3	2309.301	2112.775	2166.641	2196.239	101.551
	EXP22-4	4022.115	4439.356	3914.975	4125.482	277.051
	EXP22-5	3020.875	2980.080	2283.339	2761.431	414.542
	EXP22-6	4794.512	4892.349	4672.692	4786.518	110.046
	EXP22-7	4013.542	4231.290	4114.124	4119.652	108.979
	EXP23-1	4192.413	4353.985	4620.924	4389.107	216.404
	EXP23-2	3485.749	3423.269	3736.523	3548.514	165.791
	EXP23-3	3044.305	2939.471	3020.104	3001.293	54.890
	EXP23-4	2510.343	2114.486	2213.158	2279.329	206.057
	EXP23-5	4097.971	4004.152	3840.682	3980.935	130.206
	EXP23-6	7001.174	7030.429	6466.998	6832.867	317.189
	EXP24-1	4122.875	4368.387	3835.848	4109.037	266.539
	EXP24-2	4658.716	4896.971	4879.823	4811.837	132.883
	EXP24-3	3089.405	3227.205	3484.884	3267.164	200.745
	EXP24-4	2519.719	2397.514	2646.495	2521.243	124.497
	EXP24-5	3657.234	3666.922	3836.152	3720.103	100.618
	EXP24-6	2523.743	2402.369	2544.398	2490.170	76.736
	EXP25-1	3848.975	3638.142	3591.516	3692.878	137.179
	EXP25-2	2526.742	2937.722	2927.665	2797.376	234.430
	EXP25-3	5568.356	5791.104	5875.586	5745.015	158.715
	EXP25-4	4233.397	4225.802	4284.182	4247.794	31.741
	EXP25-5	2881.220	3010.661	2872.246	2921.376	77.453
	EXP25-6	3573.112	3674.612	3636.157	3627.960	51.244
	EXP26-1	3393.097	3419.893	3177.568	3330.186	132.848
	EXP26-2	3012.438	2997.538	2987.562	2999.179	12.519
	EXP26-3	4761.437	4685.995	4824.189	4757.207	69.194
	EXP26-4	4422.122	5003.185	4747.176	4724.161	291.215
	EXP26-5	1203.826	1293.390	981.588	1159.601	160.536
	EXP26-6	937.053	926.827	911.306	925.062	12.964
H4 GUS	pos control 1	1070.329	1061.007	1025.452	1052.262	23.682
	neg control 1	21.276	21.196	26.894	23.122	3.267
	EXP27-1	1656.323	1546.017	1474.763	1559.034	91.477
	EXP27-2	1393.067	1320.605	1344.759	1352.811	36.896
	EXP27-3	1110.233	1114.823	1119.306	1114.788	4.536
	EXP27-4	1366.667	1341.170	1361.520	1356.452	13.483
	EXP27-5	1220.474	1162.040	1198.907	1193.807	29.549
	EXP27-6	1901.258	1863.482	1909.061	1891.267	24.377
	EXP28-1	1154.724	1270.647	1200.497	1208.623	58.387
	EXP28-2	1106.723	952.794	1160.397	1073.305	107.761

	EXP28-3	1176.009	1218.829	1169.111	1187.983	26.935
	EXP28-4	1705.388	1649.750	1821.850	1725.663	87.823
	EXP28-5	1210.585	1155.420	1076.234	1147.413	67.533
	EXP28-6	1108.410	1100.700	1097.802	1102.304	5.483
	EXP29-1	1430.017	1527.597	1413.891	1457.168	61.524
	EXP29-2	810.075	846.826	911.800	856.234	51.511
	EXP29-3	357.820	386.443	334.815	359.693	25.865
	EXP29-4	1177.952	1208.904	1157.924	1181.593	25.684
	EXP29-5	1496.986	1433.234	1498.511	1476.244	37.255
	EXP29-6	824.090	776.435	743.128	781.218	40.693
	pos control 2	526.501	490.264	506.143	507.636	18.165
	neg control 2	14.626	14.391	14.191	14.403	0.218
	EXP30-1	580.683	595.491	600.000	592.058	10.106
	EXP30-2	661.352	556.066	548.243	588.553	63.166
	EXP30-3	434.751	529.261	542.371	502.128	58.717
	EXP30-4	655.853	658.978	632.418	649.083	14.516
	EXP30-5	316.588	319.940	309.382	315.303	5.395
	EXP30-6	477.304	509.026	517.402	501.244	21.151
	EXP31-1	550.983	551.397	518.045	540.142	19.138
	EXP31-2	645.690	598.244	641.237	628.390	26.202
	EXP31-3	531.332	544.963	508.454	528.249	18.449
	EXP31-4	141.241	146.473	147.262	144.992	3.272
	EXP31-5	665.082	613.601	686.958	655.214	37.661
	EXP31-6	810.887	835.516	852.694	833.032	21.014
	EXP32-1	640.355	620.050	626.759	629.055	10.346
	EXP32-2	543.266	339.258	513.506	465.343	110.202
	EXP32-3	487.976	414.685	495.506	466.056	44.647
	EXP32-4	506.310	485.424	540.517	510.750	27.814
	EXP32-5	466.818	448.338	462.323	459.160	9.637
	EXP32-6	533.745	513.447	503.021	516.738	15.624
U6 GUS	pos control	390.639	363.753	375.534	376.642	13.477
	neg control	5.055	4.974	4.904	4.978	0.075
	EXP33-1	438.242	470.937	462.374	457.184	16.954
	EXP33-2	389.962	368.399	369.962	376.108	12.023
	EXP33-3	505.645	478.730	488.806	491.061	13.598
	EXP33-4	460.226	493.243	497.429	483.633	20.379
	EXP33-5	473.940	455.706	472.321	467.323	10.093
	EXP33-6	467.584	450.485	439.527	452.532	14.140
	EXP34-1	431.753	434.226	441.582	435.854	5.113
	EXP34-2	259.416	254.580	268.096	260.698	6.848
	EXP34-3	218.021	220.396	212.005	216.807	4.325
	EXP34-4	167.914	205.264	172.079	181.752	20.468

	EXP34-5	708.100	712.572	733.764	718.145	13.710
	EXP34-6	561.701	576.809	560.287	566.265	9.158
	EXP36-1	338.171	353.590	333.122	341.628	10.663
	EXP36-2	14.145	14.275	14.250	14.223	0.069
	EXP36-3	43.009	43.073	43.835	43.306	0.459
	EXP36-4	415.832	418.046	422.289	418.722	3.281
	EXP36-5	343.693	317.016	326.046	328.918	13.568
	EXP36-6	319.791	323.222	318.329	320.448	2.512
	EXP37-1	499.724	502.603	510.864	504.397	5.783
	EXP37-2	543.921	559.165	576.782	559.956	16.445
	EXP37-3	250.720	239.888	239.417	243.342	6.394
	EXP37-4	646.273	605.459	602.816	618.183	24.363
	EXP37-6	492.908	481.491	N/A	487.200	N/A
	EXP38-1	671.895	539.419	712.697	641.337	90.591
	EXP38-2	86.019	94.739	91.929	90.896	4.451
	EXP38-3	162.434	130.536	137.559	143.510	16.761
	EXP38-4	478.806	486.698	455.594	473.699	16.169
	EXP38-5	450.333	425.250	413.224	429.602	18.934
	EXP38-6	467.692	460.547	492.345	473.528	16.683
	EXP45-1	4838.253	4364.044	4576.802	4593.033	237.521
oF 3'shble G	EXP45-2	3503.233	3606.696	3649.191	3586.373	75.071
	EXP45-3	4405.874	4620.332	4494.552	4506.919	107.762
	EXP45-4	6258.782	6042.763	5721.519	6007.688	270.343
	EXP45-5	1268.892	1827.423	1539.838	1545.384	279.307
	EXP45-6	3630.033	4458.339	3908.512	3998.961	421.495
	EXP46-1	4022.417	4011.376	4066.918	4033.570	29.403
	EXP46-2	4031.385	4175.792	3839.521	4015.566	168.693
	EXP46-3	4901.721	4042.288	4226.489	4390.166	452.492
	EXP46-4	2477.097	2682.636	2803.478	2654.404	165.012
	EXP46-5	2213.993	2712.730	2138.787	2355.170	311.931
	EXP46-6	4276.066	3369.229	4341.223	3995.506	543.349
	EXP47-1	7305.798	6517.366	6431.784	6751.650	481.811
	EXP47-2	3937.031	4208.695	4399.123	4181.616	232.233
	EXP47-3	5533.104	5990.450	5710.605	5744.720	230.574
	EXP47-4	6408.605	5778.820	5923.331	6036.919	329.900
	EXP47-5	4438.849	3609.894	3656.416	3901.720	465.749
	EXP47-6	3884.129	3620.242	3164.818	3556.396	363.881
	EXP48-1	5898.064	5926.949	4846.468	5557.160	615.647
	EXP48-2	5851.311	5913.145	3925.370	5229.942	1130.215
	EXP48-3	4132.731	3852.566	4574.298	4186.532	363.861
	EXP48-4	4021.568	4211.738	4665.067	4299.458	330.596
	EXP48-5	3051.572	3996.598	3854.416	3634.195	509.550

	EXP48-6	4307.293	4105.563	4488.334	4300.397	191.478
	EXP49-1	3176.630	3918.550	4558.493	3884.558	691.558
	EXP49-2	3832.940	3915.040	4305.121	4017.700	252.276
	EXP49-3	2369.940	3175.696	3476.722	3007.453	572.251
	EXP49-4	4288.961	3708.234	3670.594	3889.263	346.660
	EXP49-5	3761.933	2950.055	4122.539	3611.509	600.542
	EXP49-6	4973.482	5262.135	4984.818	5073.478	163.480
	EXP50-1	3266.847	2561.816	3579.996	3136.220	521.508
	EXP50-3	4104.887	4343.128	4114.243	4187.419	134.929
	EXP50-4	4995.887	4625.002	5001.435	4874.108	215.750
	EXP50-5	6008.054	6555.705	6678.904	6414.221	357.104
	EXP50-6	5790.700	6873.330	5055.692	5906.574	914.342
	EXP50-7	10997.197	7274.589	10791.469	9687.751	2092.390